THE EMISSION SPECTRUM OF SELENIUM MONOXIDE

MOHAMMAD AZAM

THE EMISSION SPECTRUM OF SELENIUM MONOXIDE

by

 Mohammad Azam

Submitted in partial fulfilment
of the requirements for the degree of Master of Science
Memorial University of Newfoundland
St. John's, Newfoundland, Canada

Department of Physics

March, 1973

CONTENTS

Page

iii

iv

LIST OF PLATES

ABSTRACT

The emission spectrum of SeO was excited in an electrodeless discharge tube containing Selenium dioxide powder by means of a high power microwave generator. Two new band systems of SeO in the photographic infrared region 10 780 - 9490 $\overset{o}{A}$ consisting of 46 bands degraded to longer wavelengths have been observed for the first time. The vibrational analysis of one band system which consists of several double-headed bands shows that it arises from the forbidden transition $b\,^1\Sigma^+ - X\,^3\Sigma^-$. The double-headed bands have been analyzed as belonging to the $^1\Sigma^+ - X\,^3\Sigma^-(F_1)$ and $^1\Sigma^+ - X\,^3\Sigma^-(F_2,F_3)$ sub-systems. The separations between the corresponding band heads of these two sub-systems are consistent with the expected value of $\sim 2\lambda$, λ $(= 86.4\ cm^{-1})$ being the splitting constant of the $^3\Sigma^-$ state derived by Barrow and Deutsch (1963) from a detailed rotational analysis of the $B\,^3\Sigma^- - X\,^3\Sigma^-$ system of SeO. The vibrational assignments are confirmed by the observed isotope band heads of ^{82}SeO, ^{80}SeO, ^{78}SeO, and ^{76}SeO. The second band system which consists of a single sequence of bands in the region 10 780 - 10 500 $\overset{o}{A}$ is tentatively assigned to the probable transition $a(^1\Delta) - X\,^3\Sigma^-$ of SeO.

The known emission spectrum of SeO in the far ultraviolet region 2490 - 1930 $\overset{o}{A}$ was photographed and a re-analysis of the bands has been presented. The re-analysis includes a fairly complete vibrational analysis of three band systems, $c(^1\Sigma^+) - b(^1\Sigma^+)$,

$C(^3\Pi)$ - X $^3\Sigma^-$ and $D(^3\Sigma^-)$ - X $^3\Sigma^-$ and a tentative vibrational analysis of two brief systems x_2 - x_1 and y_2 - y_1. The lower state of the $c(^1\Sigma^+)$ - $b(^1\Sigma^+)$ system is found to be the upper state of the $b(^1\Sigma^+)$ - X $^3\Sigma^-$ system mentioned above.

The constants of ^{80}SeO derived from these vibrational analyses are as follows (the constants for the X state are those derived by Barrow and Deutsch, 1963):

State		T_e (cm⁻¹)	ω_e (cm⁻¹)	$\omega_e x_e$ (cm⁻¹)	λ (cm⁻¹)
y_2	y_1	+47830	974	6.0	-
y_1	y_1		906	21.0	-
x_2	x_1	+46009	993	2.0	-
x_1	x_1		877	8.0	-
D $(^3\Sigma^-)$ F_2		51424	938	5.5	
F_1		51356	955	8.5	~37
C $(^3\Pi)$		50874	1034	9.3	-
c $(^1\Sigma^+)$		43509	954	13.0	-
b $(^1\Sigma^+)$		9570.7	834.9	5.5	-
a $(^1\Delta)$	T_{00}	=9518.4	-	-	-
X $^3\Sigma^-$ F_2		0.0	915.43	4.52	-
F_1		-172	914.69	4.52	λ_0=86.4

CHAPTER I

INTRODUCTION

1.1 Electronic Spectra of O_2, SO, and SeO:

The nature of the electronic states and the type of binding
of a molecule are determined mainly by the electrons in the outer-
most shells of its constituent atoms. Considering the analogous
diatomic molecules O_2, SO and SeO (formed of the sixth group elements
of the periodic table), one expects within a first approximation
similar electronic spectra because the outer most shells of each of
the elements O, S and Se contain four p electrons. The electronic
states of the symmetric molecule O_2 differ, however, from those of
SO and SeO in one or two respects. For example, its electronic
states are either even (g) or odd (u) because of the symmetry of the
nuclei and only the symmetric rotational levels occur because the
oxygen nucleus has zero spin. The relative positions of the electronic
states and the nature of the coupling between the electronic motion
and rotation of O_2, SO and SeO are dependent to a considerable extent
on the electrons of the inner shells of their constituent atoms. If
a large number of band systems for each of these analogous molecules
are discovered and analyzed, it is possible to determine the nature
of the couplings between the electronic motion and rotation of the
nuclei in their electronic states and to obtain a proper correlation
between these states.

The electronic band spectrum of O_2, both in emission and
absorption, has been extensively studied for a long period extending

over several decades. These studies have lead to great advances
in our understanding of the structure of O_2 in its electronic ground
state as well as in a large number of higher states. The number
of electronic states so far observed for O_2 is at least 10 which
have given rise to 14 band systems (see Rosen, 1970, P-423 and
the references therein). Nine of these band systems have the ground
electronic state as their common lower state. In addition, a number
of Rydberg transitions (see also Rosen, 1970) and several double
electronic transitions (see Findlay, 1970, and the references
therein) have been observed for O_2. These electronic band systems
extend from 500 $\overset{o}{A}$ in the vacuum ultraviolet to 19 100 $\overset{o}{A}$ in the near
infrared.

Compared to the large amount of spectroscopic data which
have been obtained for O_2, our knowledge of the electronic band
spectra of SO and SeO is not very extensive. Three electronic band
systems all with a common lower ground state have been observed for
SO in the spectral region 10 900 - 1900 $\overset{o}{A}$ and its structure in all the
four electronic states has been determined (Collins, 1968, 1969).
Up to 1963 only one band system has been observed and analyzed for
SeO and in 1964 four new band systems have been reported (see Section
1.2). These band systems occur in the spectral region 5100 - 1840 $\overset{o}{A}$.

The group of molecules O_2, SO and SeO have the ground
electronic configuration --- $(z\sigma)^2 (y\sigma)^2 (w\pi)^4 (x\sigma)^2 (v\pi)^2$, which
gives rise to the molecular states $X\,^3\Sigma^-$, $a\,^1\Delta$ and $b\,^1\Sigma^+$. For O_2
the forbidden band systems $a\,^1\Delta - X\,^3\Sigma^-$ and $b\,^1\Sigma^+ - X\,^3\Sigma^-$ have been

observed in absorption (Herzberg and Herzberg, 1947; Babcock and Herzberg, 1948). Recently Collins (1968) observed the b $^1\Sigma^+$ - X $^3\Sigma^-$ system for SO. Even though the a $^1\Delta$ - X $^3\Sigma^-$ transition for SO has not yet been observed, Carrington, Levy, and Miller (1966) have obtained information concerning the a $^1\Delta$ state from its electron spin resonance spectrum obtained in a gas phase reaction. The corresponding forbidden transitions are not yet discovered for SeO from its electronic spectrum. However, Carrington et al, (1969) obtained information concerning a $^1\Delta$ state of SeO just as in SO from its electron spin resonance spectrum. Further the new band systems of SeO in the far ultraviolet observed by Haranath (1964) at very low resolution deserve a closer examination at a higher resolution. A careful experimental investigation of the electronic band spectrum of SeO was therefore considered necessary. The present thesis describes the results obtained from a study of the emission spectrum of SeO in the photographic infrared and far ultraviolet regions.

1.2 Previous Work on the Electronic Band Spectrum of SeO:

(a) The B $^3\Sigma^-$ - X $^3\Sigma^-$ System:

(i) Asundi, Jan-Khan and Samuel (1936) were the first to observe the characteristic emission spectrum of SeO in the region 3950 - 3230 Å which was excited by introduction of selenium dioxide (SeO$_2$) into a bunsen flame. The spectrum was found to consist of 10 red degraded bands some of which have double heads. A tentative

vibrational analysis for these bands was proposed by these authors.

(ii) Choong-Shin Piaw (1938) photographed the emission
spectrum of SeO in the region 3950 - 3100 $\overset{o}{A}$ excited in a high voltage
transformer discharge through a slow stream of oxygen which passed
over heated selenium. The band system was found to consist of 20
double-headed red degraded bands, with the weak secondary heads lying
at wavelengths 5 to 10 $\overset{o}{A}$ shorter than those of the main heads. The
wavenumbers (cm^{-1}) of the main heads (designated as system A by
Choong-Shin Piaw) have been represented by the equation:

$$\nu = 33304.72 + \{511.00 \ (v' + \tfrac{1}{2}) - 3.50 \ (v' + \tfrac{1}{2})^2\}$$
$$- \{907.08 \ (v'' + \tfrac{1}{2}) - 4.61 \ (v'' + \tfrac{1}{2})^2\} \ ,$$

and those of the weak heads (designated as system B by him) have been
represented by the equation:

$$\nu = 33375.92 + \{519.24 \ (v' + \tfrac{1}{2}) - 3.42 \ (v' + \tfrac{1}{2})^2\}$$
$$- \{907.08 \ (v'' + \tfrac{1}{2}) - 4.61 \ (v'' + \tfrac{1}{2})^2\} \ .$$

(iii) The strong emission bands of this system of SeO
which was excited in a radio-frequency discharge through selenium
vapor in the presence of oxygen were photographed by Barrow and
Deutsch (1963) under the high dispersion of a 6.65 m grating spectro-
graph in the second order, giving a reciprocal dispersion of about
0.5 $\overset{o}{A}$/mm. These authors have carried out the rotational analysis
for 9 bands and ascribed the transition A $^3\Sigma^-$ - X $^3\Sigma^-$, which is

hereafter referred to as $B\ ^3\Sigma^-$ - $X\ ^3\Sigma^-$ because this system is analogous to the transitions $B\ ^3\Sigma^-$ - $X\ ^3\Sigma^-$ in O_2 (Schumann-Runge System) and in SO. The splitting constants λ'' and λ' of the ground and upper $^3\Sigma^-$ states of system B-X were found to be very large. The double-headed appearance of the bands was explained on the basis of the splitting of each band of the $^3\Sigma^-$ - $^3\Sigma^-$ system into three sub-bands, two of them due to F_2-F_2 and F_3-F_3 transitions which lie very close and one due to F_1-F_1 transitions which are well separated by an amount ~$2(\lambda'-\lambda'')$ from the former. The molecular constants of the $X\ ^3\Sigma^-$ and $B\ ^3\Sigma^-$ states obtained by Barrow and Deutsch (1963) are summarized in Table I.

(iv) Haranath (1964) reinvestigated the emission spectrum of SeO using a radio-frequency electrodeless discharge from a high power valve oscillator through flowing vapor of SeO_2 and obtained 25 additional double-headed bands of the $B\ ^3\Sigma^-$ - $X\ ^3\Sigma^-$ system of SeO in the region 5100 - 3900 $\overset{o}{A}$ under medium dispersion. The assignment of the vibrational quantum numbers to these bands was confirmed from the observed isotopic heads due to ^{80}SeO and ^{78}SeO.

(b) <u>Ultraviolet Systems:</u>

Haranath (1963) also studied the emission spectrum of SeO in the region 2400 - 1800 $\overset{o}{A}$ and observed over 40 bands under low dispersion. These bands were analyzed into the following four systems: $C - X\ ^3\Sigma^-$, $D - x$, $F - x$ and $E - X\ ^3\Sigma^-$. The x state was assumed to be the $^1\Sigma^+$ state belonging to the ground state electron configuration. As can be seen later in this thesis, the ultraviolet bands of

TABLE I

Constants (in cm^{-1}) of the $B\ ^3\Sigma^- \rightarrow X\ ^3\Sigma^-$ System of SeO

State		T_{oo}	ω_e	$\omega_e x_e$	B	α	$r(\overset{o}{A})$	λ_o
$B\ ^3\Sigma^-$	F_2	34012.2	$G_{\frac{1}{2}} = 517.7$		$B_o = 0.3391$	-	$r_o = 1.931$	51
	F_1	33910	522.3	3.9	$B_o = 0.3332$	-		
$X\ ^3\Sigma^-$	F_2	0.0	915.43	4.52	$B_e = 0.4705$	0.0033		
	F_3	0.04	915.43	4.52	$B_e = 0.4762$	0.0032	$r_e(F_2) = 1.640$	86.4
	F_1	-172	914.69	4.52	$B_e = 0.4655$	0.0032		

SeO have been photographed at relatively higher dispersion and re-analyzed in the present work.

1.3 The Present Study of the Emission Spectrum of SeO:

The emission spectrum of SeO was excited in an electrodeless quartz discharge tube containing selenium dioxide powder by means of a high power microwave generator. Two new band systems of SeO in the photographic infrared region 10 780 - 9490 $\overset{o}{A}$ were observed for the first time. The vibrational analysis of one band system which consists of several double-headed bands degraded to longer wavelengths reveals that it arises from the forbidden transition $b \ ^1\Sigma^+ - X \ ^3\Sigma^-$. The double-headed bands have been analyzed as belonging to the $^1\Sigma^+ - X \ ^3\Sigma^-(F_1)$ and $^1\Sigma^+ - X \ ^3\Sigma^-(F_2,F_3)$ sub-systems. The vibrational assignments are supported from the observed band heads of the isotopes ^{82}SeO, ^{80}SeO, ^{78}SeO, and ^{76}SeO. The other band system which consists of a single sequence of bands also degraded to longer wavelengths in the region 10 780 - 10 500 $\overset{o}{A}$ is tentatively assigned to the probable transition $a \ ^1\Delta - X \ ^3\Sigma^-$.

The emission spectrum of SeO in the far ultraviolet region 2490 - 1930 $\overset{o}{A}$ has been reinvestigated. Altogether 43 bands have been photographed and re-analyzed. The re-analysis includes a fairly complete vibrational analysis of three band systems $c \ (^1\Sigma^+) - b \ (^1\Sigma^+)$, $C \ (^3\pi) - X \ ^3\Sigma^-$ and $D \ (^3\Sigma^-) - X \ ^3\Sigma^-$ and a tentative vibrational analysis of two brief systems $x_2 - x_1$ and $y_2 - y_1$. The lower state of the $c \ (^1\Sigma^+) - b \ (^1\Sigma^+)$ system is found to be the upper state of the $b \ (^1\Sigma^+) - X \ ^3\Sigma^-$ system discussed above.

CHAPTER 2

EXPERIMENTAL TECHNIQUE

In the present chapter, the apparatus used for the excitation of the spectrum of selenium monoxide and the experimental procedure adopted in photographing and measuring the spectrum will be described briefly.

2.1 Experimental Apparatus:

(a) Microwave Generator:

The emission spectrum of selenium monoxide was excited in a quartz discharge tube containing selenium dioxide powder by radiation obtained from the microwave power generator model PGM - 100 supplied by the Raytheon Company, Mass., U.S.A. The experimental set up of the microwave generator and its accessories are shown schematically in Fig. 1, where PG is the microwave generator, F is its filter unit, G is the waveguide, H is the horn and P is the probe. Also shown in Fig. 1 is the radiation cage C which encloses the horn, the discharge tube D and the metallic reflector R. The constructional details of the waveguide and the horn have been described in a greater detail by Ali (1969).

The microwave generator is a fixed frequency, air-cooled, CW-type magnetron oscillator. The magnetron is supplied with a full wave rectifier power unit in which a magnetic regulator maintains the average anode current constant. The power output from the

CHAPTER 2

EXPERIMENTAL TECHNIQUE

In the present chapter, the apparatus used for the excitation of the spectrum of selenium monoxide and the experimental procedure adopted in photographing and measuring the spectrum will be described briefly.

2.1 Experimental Apparatus:

(a) <u>Microwave Generator:</u>

The emission spectrum of selenium monoxide was excited in a quartz discharge tube containing selenium dioxide powder by radiation obtained from the microwave power generator model PGM - 100 supplied by the Raytheon Company, Mass., U.S.A. The experimental set up of the microwave generator and its accessories are shown schematically in Fig. 1, where PG is the microwave generator, F is its filter unit, G is the waveguide, H is the horn and P is the probe. Also shown in Fig. 1 is the radiation cage C which encloses the horn, the discharge tube D and the metallic reflector R. The constructional details of the waveguide and the horn have been described in a greater detail by Ali (1969).

The microwave generator is a fixed frequency, air-cooled, CW-type magnetron oscillator. The magnetron is supplied with a full wave rectifier power unit in which a magnetic regulator maintains the average anode current constant. The power output from the

Fig. 1. Schematic Diagram of the Microwave Power Generator, its

Accessories, the Discharge Tube and the Radiation Cage.

generator thus remains virtually constant through normal line

fluctuations and variations of magnetron impedance with load and

life. A power output having a modulation of about 10% in the

detected R.F. envelope of the microwave generator is provided by

the use of the filter unit F. With the filter in, the output power

range of the microwave generator is 250 to 800 watts at a frequency

of 2450 ± 50 MHz.

Special care was taken to avoid the hazards of microwave

radiation in the laboratory. The horn H of the microwave generator,

the quartz discharge tube D and the metallic reflector R were enclosed

in a rectangular radiation cage C (Fig. 1) of size 40" x 40" x 29"

made of copper screen of mesh size 0.10 cm. x 0.15 cm. A rubber

pad was placed on the bottom surface of the cage and bricks made of

clay were placed along the walls of the cage in order to absorb

the scattered radiation inside the cage. An air conditioner was

used in the room containing the experimental set up to reduce the

heat produced by the microwave generator and the bunsen burner which

was used to heat the discharge tube.

(b) Discharge Tube:

The electrodeless quartz discharge tube used in the present

investigation was 18" long and 1" in diameter and is shown in Fig. 2.

About 40 to 50 grams of selenium dioxide supplied by the British

Drug Houses Ltd., England or Anachemia Chemicals Ltd., Montreal or

Alpha Inorganics Ventron, Beverly, Mass., U.S.A. was placed in the

WINDOW

DISCHARGE TUBE

TO VAC.
SYSTEM

LIQUID N₂ TRAP
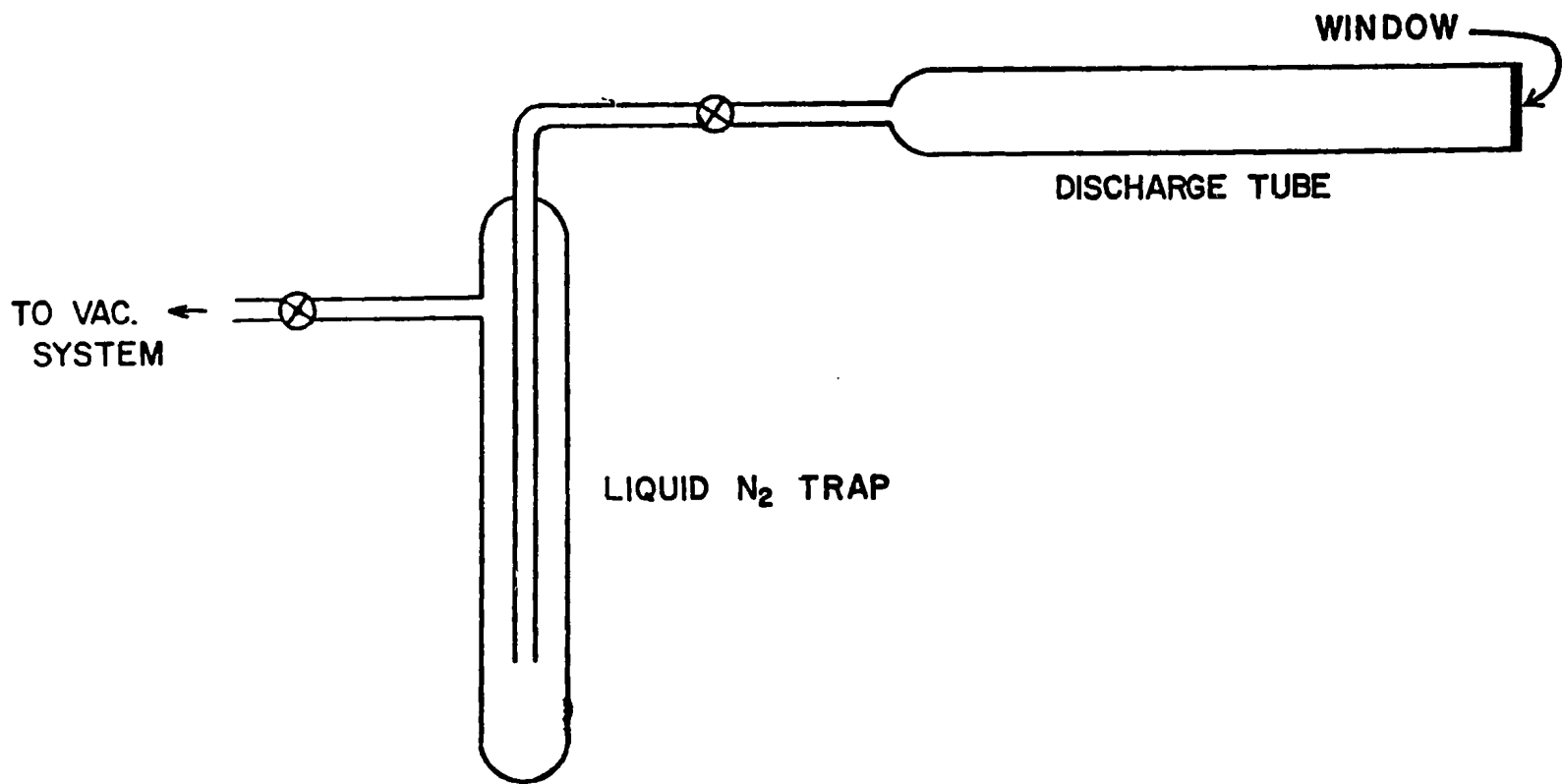
Fig. 2.   Discharge Tube and Liquid Nitrogen Trap .

discharge tube. A circular quartz window W, 2 mm in thickness, was fused at one end of this tube. The other end of the tube was connected to a pyrex tubing through a graded seal. The pyrex tube was then joined to a liquid nitrogen trap through a pyrex stopcock and finally to a high vacuum pumping system. The dissociation products of the discharge coming out through the pumping system were properly exhausted from the room.

(c) <u>Mechanism of Electrical Discharges</u>:

In all types of electrical discharge tubes, electric energy is converted into light by transformation of electric energy into the translational energy of free electrons which in turn is converted into radiation as a result of some kind of collision process. The basic process involved in producing and maintaining an electric discharge in any discharge tube is as follows: Free electrons in an evacuated discharge tube are first accelerated by the electric energy from a device such as a microwave power generator, a tesla coil, a high frequency valve oscillator, or a high voltage d.c. or a.c. power supply unit. The kinetic energy of the accelerated free electrons is then transformed into the internal energy of the atoms or molecules in the discharge tube due to collisions. In this way, the atoms and molecules are excited to their higher internal energy states. For molecules, this internal energy could be electronic, vibrational and rotational whereas for atoms it is only electronic in nature.

Higher internal energy states of atoms and molecules are inherently unstable and the excited atom or molecule gives up energy by dropping into a lower state with the emission of electromagnetic radiation of frequency ν such that $h\nu$ (h being the Planck's constant) is equal to the energy difference between the two states. The free electrons are again accelerated by the external electric energy and their translational energy is transformed into the internal energy by the atoms or molecules and the whole process is repeated.

An important result of the investigation of molecular spectra by electrical discharges is proof of the physical existence of a large number of molecules such as CH, OH, C_2, He_2, etc., which were previously unknown in chemistry. In the present study, the excitation of the SeO molecule in a discharge tube containing SeO_2 is an example for this type of molecules. The characteristic emission spectrum of SeO obtained under continuous evacuation of the discharge tube shows clearly that SeO_2 in the discharge tube gives rise to SeO, oxygen and possibly some free selenium. In the present experiment, it was found necessary to initiate the discharge with the help of a tesla coil while irradiating the discharge tube with the microwave power generator.

(d) <u>Bausch and Lomb Dual Grating Spectrograph:</u>

The emission spectrum of SeO was photographed on a Bausch and Lomb Dual Grating Spectrograph. A schematic diagram of the optical

arrangement of the spectrograph is shown in Fig. 3. Light from

a discharge tube is incident on a variable slit. After being

reflected by a plane mirror, it is then focused on to one of the

gratings #1 or #2 by a spherical mirror having a radius of

curvature of 2 m and a numerical aperture of f/15.5. The light

dispersed by the grating is again incident on the spherical mirror

which then focuses it on to a photographic plate. Spectra in

juxtaposition were obtained with the help of a Hartmann diaphragm

in front of the slit. The plate holder can be moved up or down

either manually or automatically. The two plane gratings were

mounted back to back in a rotatable turret. Each of them has

a ruled width of 128 mm and a groove length of 102 mm. One

of them has 1200 grooves/mm and the other has 600 grooves/mm.

The former was used throughout the present work. The infrared

spectrum of SeO was photographed in the first order of the

grating and its spectrum in the ultraviolet region was photographed

in the first and the third orders. The reciprocal dispersions

obtained with the grating are 3.29 $\overset{o}{A}$/mm at 10 000 $\overset{o}{A}$ in the

first order, and 4.13 $\overset{o}{A}$/mm and 1.29 $\overset{o}{A}$/mm at 2100 $\overset{o}{A}$ in the

first and the third order respectively. The slit width was maintained

in the range 0.17 mm to 0.30 mm depending on the intensity of

the band system being photographed. The following are the

specifications of the grating with 1200 grooves/mm as supplied

Gratings

#1 #2

Turret Axis

Photographic Plate

Mirror

Variable
Slit

Light From the
Discharge Tube

Spherical
Mirror
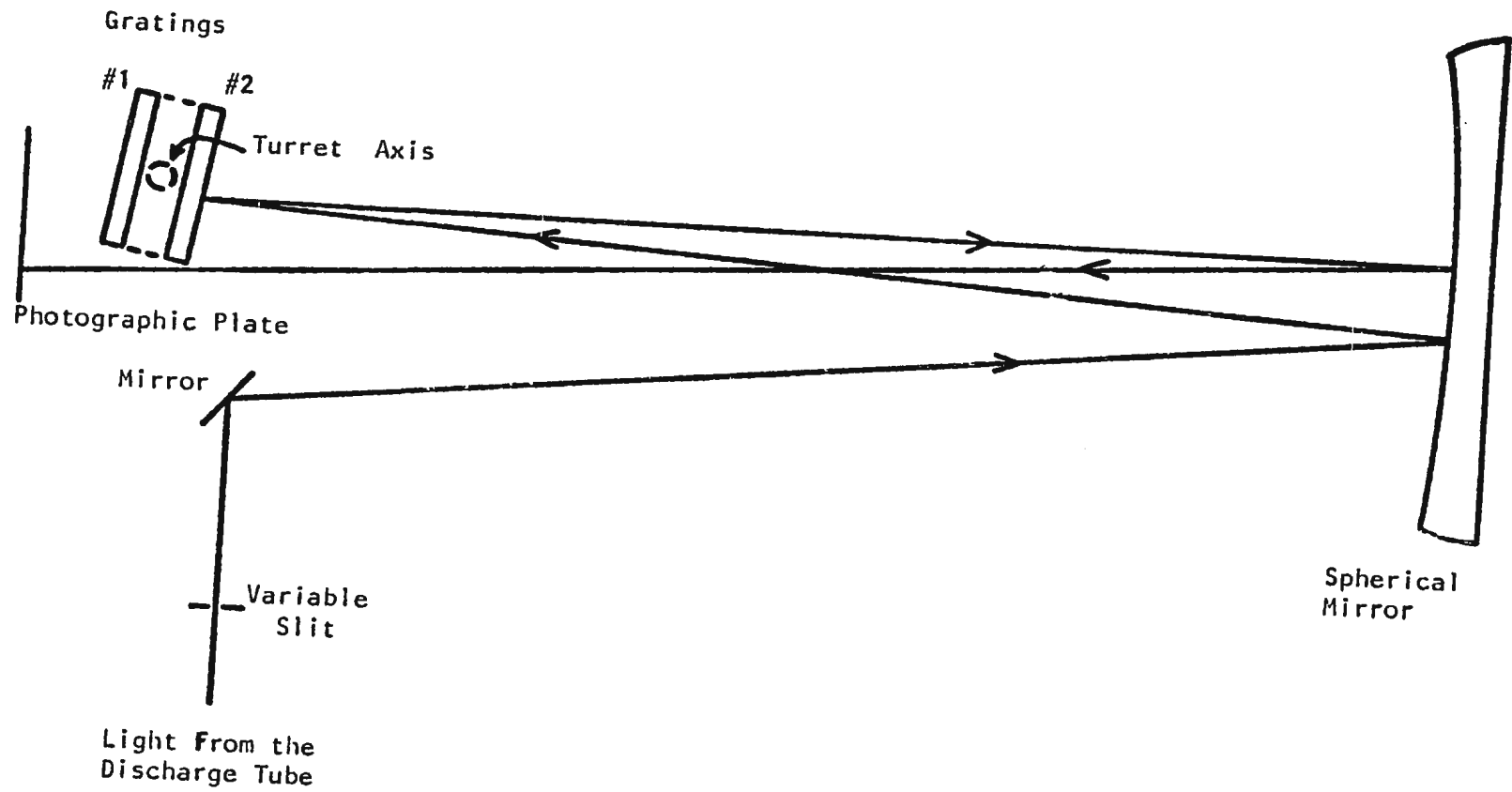
Fig. 3. Optical Arrangement of the Spectrograph .

by the manufacturers:

Blazed wave length:	1.0 micron (first order)
Blaze angle:	36° 52'
Resolving power (for infinitesimal slit width):	70% of the theoretical value (153 600 in the first order)
Efficiency:	62% at 9000 Å 66% at 1.0 micron 70% at 1.1 microns
Ghost intensity:	1.0% of the parent line in the second order at 5461 Å

The experimental resolving power $\frac{\lambda}{\Delta\lambda}$ in the present work, for example, at 10 000 Å with a slit width of 0.30 mm is 10 000 Å/((3.29 Å/mm) x 0.30 mm) $\simeq 10^4$, which corresponds to a spectral resolution of 1 Å. The reason for using wider slits is that the intensities of the band systems under investigation are rather low.

2.2 Experimental Procedure:

The quartz discharge tube containing SeO_2 powder was optically aligned with the slit of the spectrograph so that the light from the discharge tube fills the collimator of the spectrograph

uniformly (see Fig. 3). The discharge tube was first evacuated to a pressure of approximately 5×10^{-5} torr. The central part of the discharge tube was then heated by a special bunsen burner giving a flame over a length of 10". With the radiation cage C (Fig. 1) closed, the discharge tube was irradiated with the microwave power from the microwave generator. It was found necessary to excite the discharge tube initially with a tesla coil. The characteristic color of the SeO discharge was bluish white. Maximum intensity of the discharge was obtained by adjusting the position of the reflector R (Fig. 1). Condensation of the discharge vapors on the window and in the graded seal extension of the discharge tube was prevented by the use of low flames from two separate bunsen burners. With continuous evacuation, the discharge could be maintained without interruption for sufficiently long periods up to 20 hours or more. The anode current of the microwave generator was kept at 260 ma.

The position of the metallic reflector R adjusted to obtain the maximum intensity of the discharge corresponds also to the lowest voltage standing wave ratio (VSWR), to be referred hereafter as ρ . A rough estimate of ρ was made using a probe P (Fig. 1) as follows: The probe connected to one of the arms of a Wheatstone Bridge Circuit was moved in the slot S of the waveguide. A plot of the resistances required to balance the bridge circuit versus the probe distances along the waveguide gave a curve similar to a sine curve with a few maxima and minima.

the
Since/probe itself was not calibrated, the square roots of the
ratios between the resistances corresponding to maxima and minima
of voltage were assumed to represent ρ's . The values of ρ
obtained in this way varied from 1.26 to 1.31. The power
received P_r was calculated from the equation

$$(2-1) \qquad P_r = P_a \left(4\rho/(1 + \rho)^2\right)$$

where P_a is the available power which was taken from the calibration
curve obtained previously by Hynes (1968) for the present microwave
generator by a water load method. From this curve it was found
that the power available from the microwave generator corresponding
to the anode current maintained at 260 ma was 755 watts. Using
a value of 1.31 for ρ , the corresponding value of P_r was
found to be 740 watts.

The spectra in the infrared region 10 800 - 9400 $\overset{o}{A}$ were
photographed in the first order of the grating with 1200 grooves/mm
on hypersensitized Kodak I-Z plates. Kodak I-Z plates were
hypersensitized by bathing them in dilute ammonium hydroxide (2 parts
of 28% NH_4OH and 100 parts of water) for three minutes. They were
then immersed in methyl alcohol for two minutes and were at once
dried rapidly by cold air from a fan. The exposure times ranged
from 10 to 14 hours with the slit width maintained at 0.3 mm.
Kodak Wratten filter #70 was used to eliminate the overlapping of
higher order spectra. Second and third order spectral lines from
a d.c. iron arc, operated at 125 volts and 4 amperes which were

photographed in the juxtaposition to the SeO spectrum served as
wavelength standards. It is to be noted that when no filter was
used for the iron arc spectra only the second and third order
lines were recorded because the first order iron lines are very
weak and the I-Z plates are not sensitive to the fourth and
higher orders.

Kodak SWR plates were used to record the spectra in
the ultraviolet region 2400 - 1800 $\overset{o}{A}$. The spectra were photographed
in the first and third orders of the grating using a slit width
of 0.2 mm. D.C. copper arc lines were used as standard wave-
lengths in this region. The exposure times for the first and the
third order spectra of SeO were approximately 7 and 5 hours,
respectively. For the third order spectra, a 5 cm chlorine gas
cell prepared by the author (see section 2.4) was used as a filter
to eliminate overlapping of second order spectra. Kodak SWR
plates are not sensitive to the overlapping first order spectra.

2.3 Measurement of Spectra:

A linear comparator Model M1205C supplied by the
Gaertner Optical Company, Chicago, Illinois, U.S.A., was used to
measure the spectra. The least count of the comparator is 0.001 mm.
However, the readings were estimated correct to 0.0001 mm. The
comparator readings d of the band heads and of the standard iron
(or copper) arc lines in a given spectral region were obtained from
the spectral plates. The wavelengths λ_{air} of several iron (or copper)

arc lines were used to determine the constants a_0, a_1, and a_2
of the equation

(2-2) $\lambda_{air} = a_0 + a_1 d + a_2 d^2$,

by the method of a least squares fit. The accuracy of these
constants was tested by calculating the wavelengths of the other
standard lines in the same spectral region whose d values had
been measured. The accuracy of measurement for sharp lines in
the first order spectra in the infrared region is much better than
0.02 $\overset{o}{A}$ whereas it is about 0.03 $\overset{o}{A}$ and 0.01 $\overset{o}{A}$ for the first
and third order spectra in the ultraviolet region 2300 - 1900 $\overset{o}{A}$.
However, the accuracy of measurement for diffuse band heads is
considerably less. The wavelengths of the band heads of the SeO
spectrum were calculated from Eq.(2-2). Edlen's (1953) formula
for the refractive index, n, of air, i.e.,

(2-3) $n = 1 + 6432.8 \times 10^{-8} + \dfrac{2949810}{146 \times 10^8 - \nu^2}$

$+ \dfrac{25540}{41 \times 10^8 - \nu^2}$,

where

$\nu(cm^{-1}) = \dfrac{10^8}{n\lambda_{air}(\overset{o}{A})}$,

was used to convert wavelengths in air λ_{air} to vacuum wavenumbers
ν . An iterative method was employed to do the computations on an
IBM 370 computer and the iteration was continued until the absolute

difference between the successive values of ν was $\leq 10^{-10}$ cm^{-1}.
Hewlett-Packard calculator Model 9100A was used for some
calculations.

2.4 A Chlorine Filter Which Absorbs The Near Ultraviolet Radiation and Transmits The Far Ultraviolet:

When a grating spectrograph is used to photograph a
spectrum in a specified spectral region, it is often necessary to
filter out the unwanted spectral region(s) which overlap the
region of interest. Many glass filters which absorb the ultraviolet
and transmit the visible radiation serve the purpose very well in
a number of problems. However, the glass filters cannot be used
in certain cases in which ultraviolet radiation in a specific
region is to be transmitted and some other unwanted ultraviolet
radiation is to be filtered out. For example, if one wants to
photograph the spectral region 2500 - 1900 $\overset{o}{A}$ in the third order,
it overlaps the second order region 3750 - 2700 $\overset{o}{A}$ and there is
no commercial glass filter which removes the unwanted second order
region and transmits the required third order region. /$\overset{A}{}$ Chlorine
gas filter was quoted to do this function admirably (see Wood, 1952).
While photographing the SeO spectrum in the far ultraviolet in
the third order of the Bausch and Lomb Dual Grating Spectrograph,
the corresponding second order overlapping region was filtered out
by a chlorine gas filter which was prepared by the author. The
details of preparation of the same are given below.

A quartz cell G, 5 cm long, 2.5 cm in diameter and having a freeze-out finger F 2.5 cm long, was connected by means of a graded seal tube E to a pyrex gas handling system through a stopcock V_1 as shown in Fig. 4. The gas handling system consists of a liquid nitrogen trap T and a mercury manometer M and was connected to a chlorine cylinder C through a valve V and to a vacuum pump through T. V_2 and V_3 are stopcocks. The system was first evacuated and the quartz cell was then filled with chlorine at a pressure of one atmosphere. With the stopcock V_1 closed, the chlorine gas was first frozen in F by cooling the same in liquid nitrogen and the gas cell (G) was then sealed at E. The transmission curve for the resulting chlorine gas filter obtained on a Perkin-Elmer Model 202 UV-Visible Spectophoto-meter is given in Fig. 5. As can be seen from this figure, the filter has ~80% transmission below 2500 $\overset{o}{A}$ and its cutoff region is 2800 - 3900 $\overset{o}{A}$. Its transmission above 4300 $\overset{o}{A}$ is ~80%.

Narrow band interference filters have very low transmission in the far ultraviolet region and are not recommended for the present type of work.

TO VACUUM PUMP
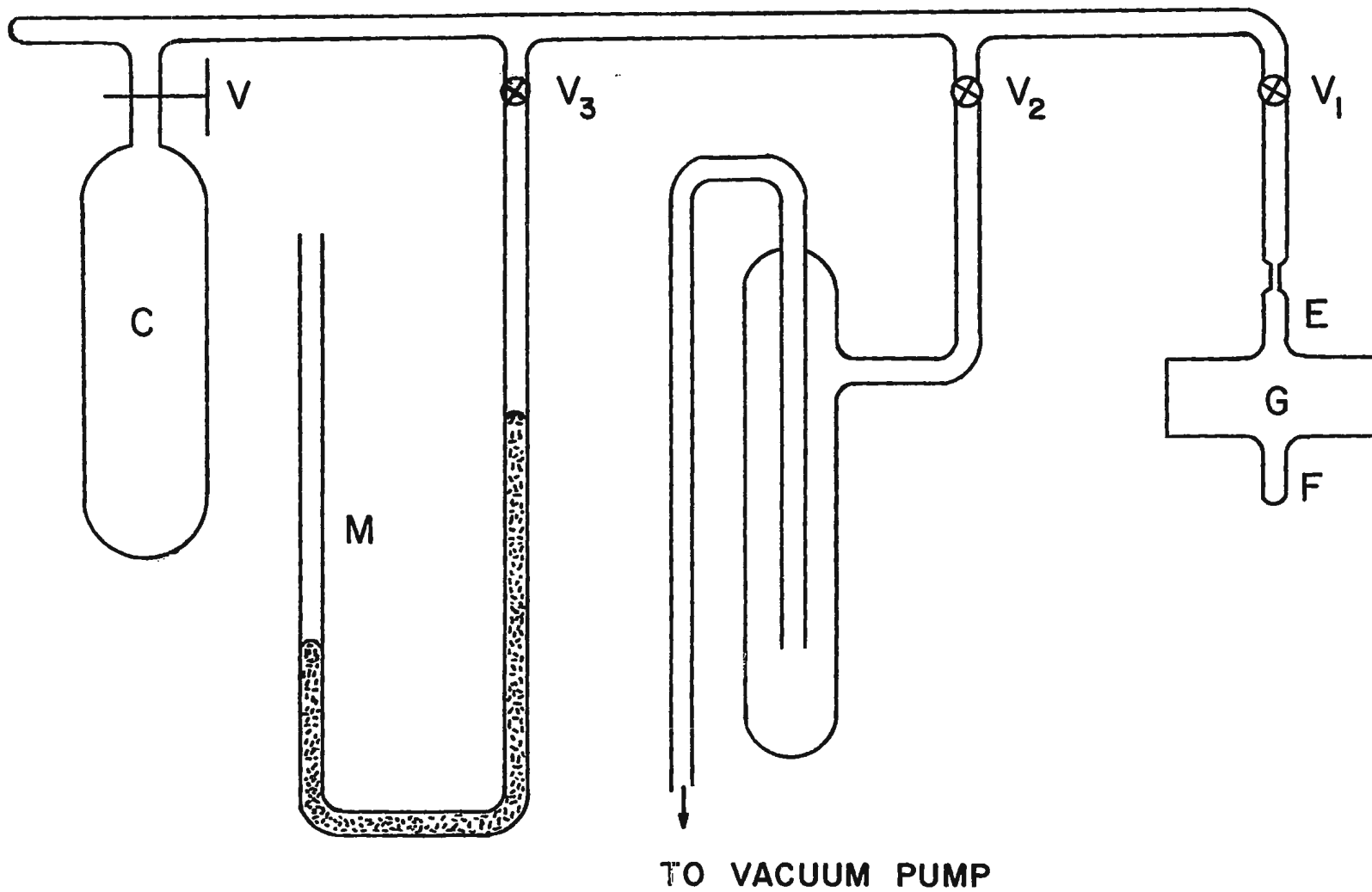
Fig. 4. Experimental Set Up For the Preparation of a Chlorine Gas Filter .
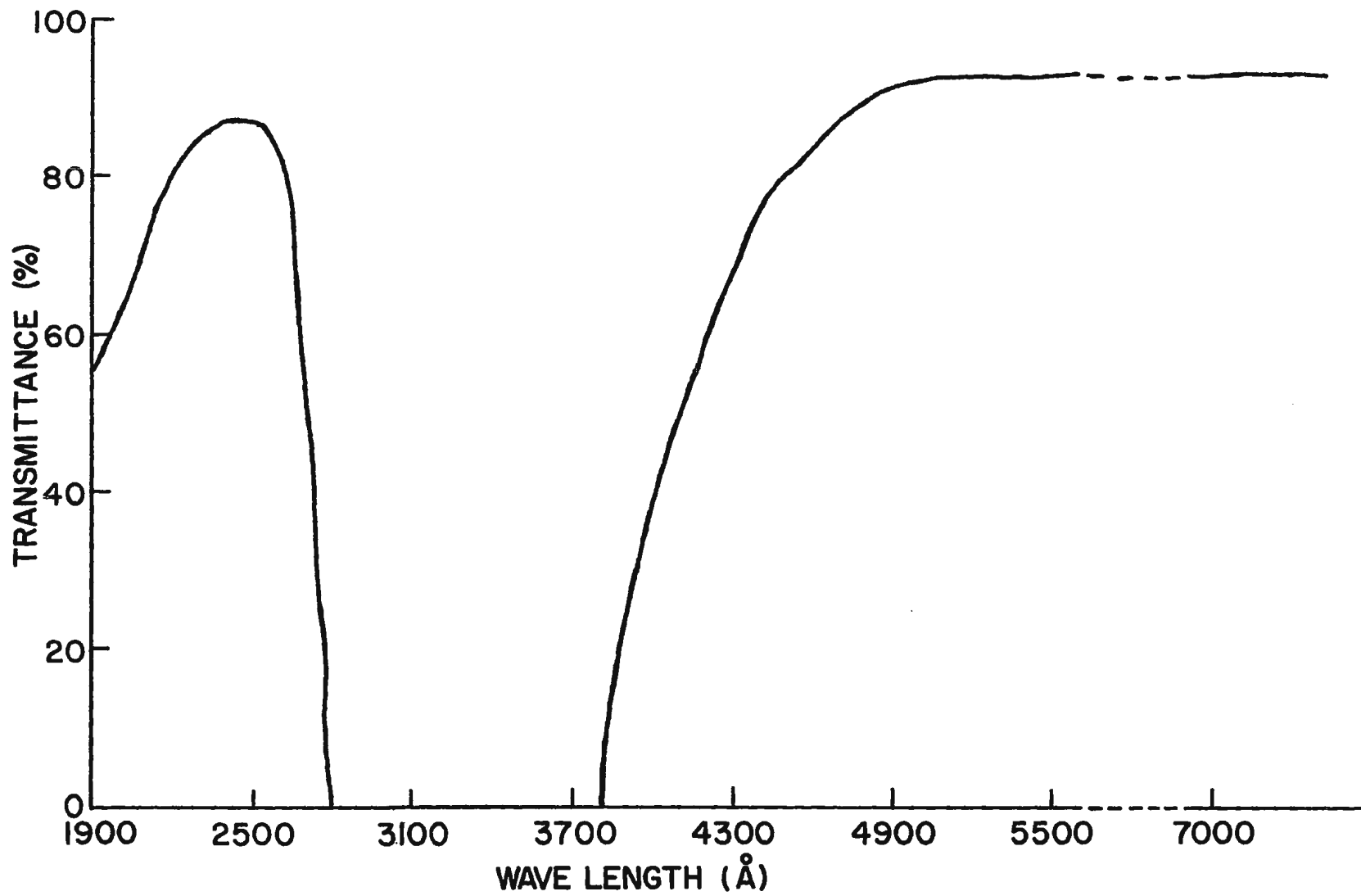
Fig. 5. Transmittance Curve of the Chlorine Gas Filter .

CHAPTER 3

THE NEW EMISSION SPECTRUM OF SeO IN THE PHOTOGRAPHIC INFRARED

In the previous chapter, the method of excitation
of the emission spectrum of SeO, the details of the spectrograph
used, and the experimental procedure followed in photographing
and measuring the spectrum are described in detail. In the present
chapter, the new experimental data obtained in the photographic
infrared region and the details of the vibrational analysis of
two new band systems, (i) b $^1\Sigma^+$ - X $^3\Sigma^-$ and (ii) (a $^1\Delta$) - X $^3\Sigma^-$
will be presented. In Section 3.1, a brief resume of the expressions
used in the vibrational analysis is given and the rest of the
chapter is devoted to the results and discussion.

3.1 Resume of the Expressions used in the Vibrational Analysis
     of the Electronic Band Systems:

The total spectral term in wavenumber unit (cm^{-1}) of a
state in a diatomic molecule, neglecting its translational and
nuclear spin energies, is given by

(3-1) $T = T_e + G(v) + F(J)$,

where T_e is the electronic term, $G(v)$ is the vibrational term,
v being the vibrational quantum number, and $F(J)$ is the rotational
term, J being the rotational quantum number. In the above equation,
T_e for the electronic states with multiplicity greater than zero

is given by

$$(3\text{-}2) \quad T_e = T^0 + A\Lambda\Sigma \ ,$$

where T^0 is the electronic energy if the spin is neglected, Λ is the quantum number of the electronic orbital angular momentum along the internuclear axis (states with $\Lambda = 0, 1, 2\ldots\ldots$ are called $\Sigma, \Pi, \Delta, \ldots\ldots$ states), Σ^* is the component of the resultant spin in the same axis and A is the spin coupling constant. The vibrational term $G(v)$ is expressed as

$$(3\text{-}3) \quad G(v) = \omega_e \ (v + \tfrac{1}{2}) - \omega_e x_e \ (v + \tfrac{1}{2})^2 + \omega_e y_e \ (v + \tfrac{1}{2})^3 + \ldots\ldots$$

If we neglect rotation in Eq.(3-1) and the cubic and higher order terms in Eq. (3-3), the wavenumber $\nu_{v',v''}$ corresponding to a transition between an upper state T' and a lower state T" is represented by

$$
\begin{aligned}
(3\text{-}4) \quad \nu_{v',v''} &= T' - T'' \\
&= (T'_e - T''_e) + G' \ (v') - G'' \ (v') \\
&= \nu_e + \omega'_e \ (v' + \tfrac{1}{2}) - \omega'_e x'_e \ (v' + \tfrac{1}{2})^2 \\
&\quad - \{\omega''_e \ (v'' + \tfrac{1}{2}) - \omega''_e x''_e \ (v'' + \tfrac{1}{2})^2\} \ .
\end{aligned}
$$

---

* In standard spectroscopic rotation, the symbol Σ represents both an electronic state characterized by $\Lambda = 0$ and also the projection of S along the internuclear axis.

Here $\nu_e (=T'_e - T''_e)$ is the system origin which is a constant for the given system. The interval between the values $G(v')$ and $G(v'')$ of a given electronic state (omitting again the cubic term in Eq. (3-3)) is given by

$$(3-5) \qquad \Delta G_{v+\frac{1}{2}} = G\,(v+1) - G(v)$$
$$= \omega_e - 2\omega_e x_e\,(v+1)$$
$$= (\omega_e - \omega_e x_e) - 2\omega_e x_e\,(v + \tfrac{1}{2}).$$

The second differences are given by

$$(3-6) \qquad \Delta^2 G_{v+1} = G_{v+3/2} - G_{v+\frac{1}{2}} = -2\omega_e x_e.$$

The wave number $\nu^i_{v',v''}$ of an isotope molecule in a given band system can be written as

$$\nu^i_{v',v''} = \nu_e + \rho\,\omega_e\,(v' + \tfrac{1}{2}) - \rho^2\,\omega'_e x'_e\,(v' + \tfrac{1}{2})^2 + \ldots\ldots$$
$$- \{\rho\,\omega''_e\,(v'' + \tfrac{1}{2}) - \rho^2\,\omega''_e x''_e\,(v'' + \tfrac{1}{2})^2 + \ldots\},$$

where $\rho = (\mu/\mu^i)^{\frac{1}{2}}$, μ being the reduced mass of the normal molecule and superscript i representing the isotope molecule. The isotope shift is represented by the relation,

$$(3-7) \qquad \Delta\nu = \nu_{v',v''} - \nu^i_{v',v''}$$
$$= (1 - \rho)\,\{\omega'_e\,(v' + \tfrac{1}{2}) - \omega''_e\,(v'' + \tfrac{1}{2})\}$$
$$- (1 - \rho^2)\,\{\omega'_e x'_e\,(v' + \tfrac{1}{2})^2 - \omega''_e x''_e\,(v'' + \tfrac{1}{2})^2\} + \ldots\ldots$$

3.2 New Emission Systems of SeO in the Near Infrared Region:

In the spectral region 10 765 - 9490 $\overset{o}{A}$, two band systems of SeO consisting of 46 band heads degraded to longer wavelengths have been observed for the first time. The general appearance of the bands is shown in the spectrograms (a), (b), (c) and (d) in Plate I. As described in Chapter 2, these SeO band systems excited in a discharge tube containing SeO_2 by a microwave power generator were photographed on a Bausch and Lomb grating spectrograph in the first order having a dispersion of 3.3 $\overset{o}{A}$/mm. The slit width was maintained at 0.3 mm. Hypersensitized Kodak I-Z plates were used. Second and third order d. c. iron arc lines were used as wavelength standards. Spectra were measured on a Gaertner linear comparator. The accuracy of measurements for sharp bands is much better than 0.02 $\overset{o}{A}$.

One of the two systems of SeO which has been identified as $b\ ^1\Sigma^+ - X\ ^3\Sigma^-$ is better developed than the second system which consists of only one sequence. The second system may probably arise from the transition $a\ ^1\Delta - X\ ^3\Sigma$.

3.3 The b - X System:

(a) Vibrational Analysis:

The b - X system of SeO is shown in Plate II(a) and II(b). The analysis of this band system was not entirely straight forward because a part of its region is overlapped by a second system

3 x 3608.68 Å   3 x 3500.57 Å

Fe arc
(a)

3 x 3500.57 Å   3 x 3389.75 Å

(b)

3 x 3406.81 Å   3 x 3298.74 Å

(c)

3 x 3280.27 Å   3 x 3165.01 Å

(d)
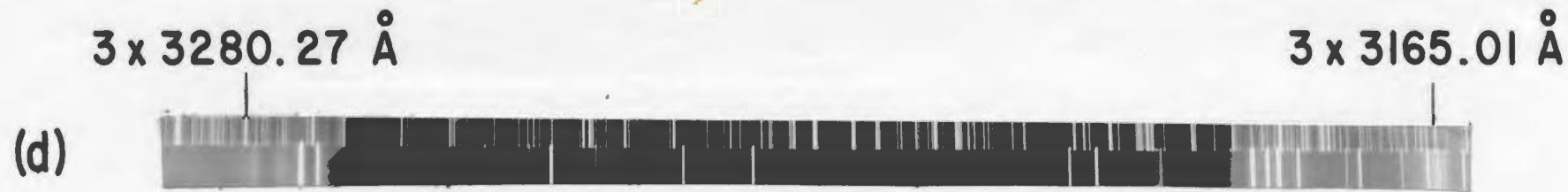
Plate I. The Emission Spectrum of SeO in the Region 10 780 - 9490 Å
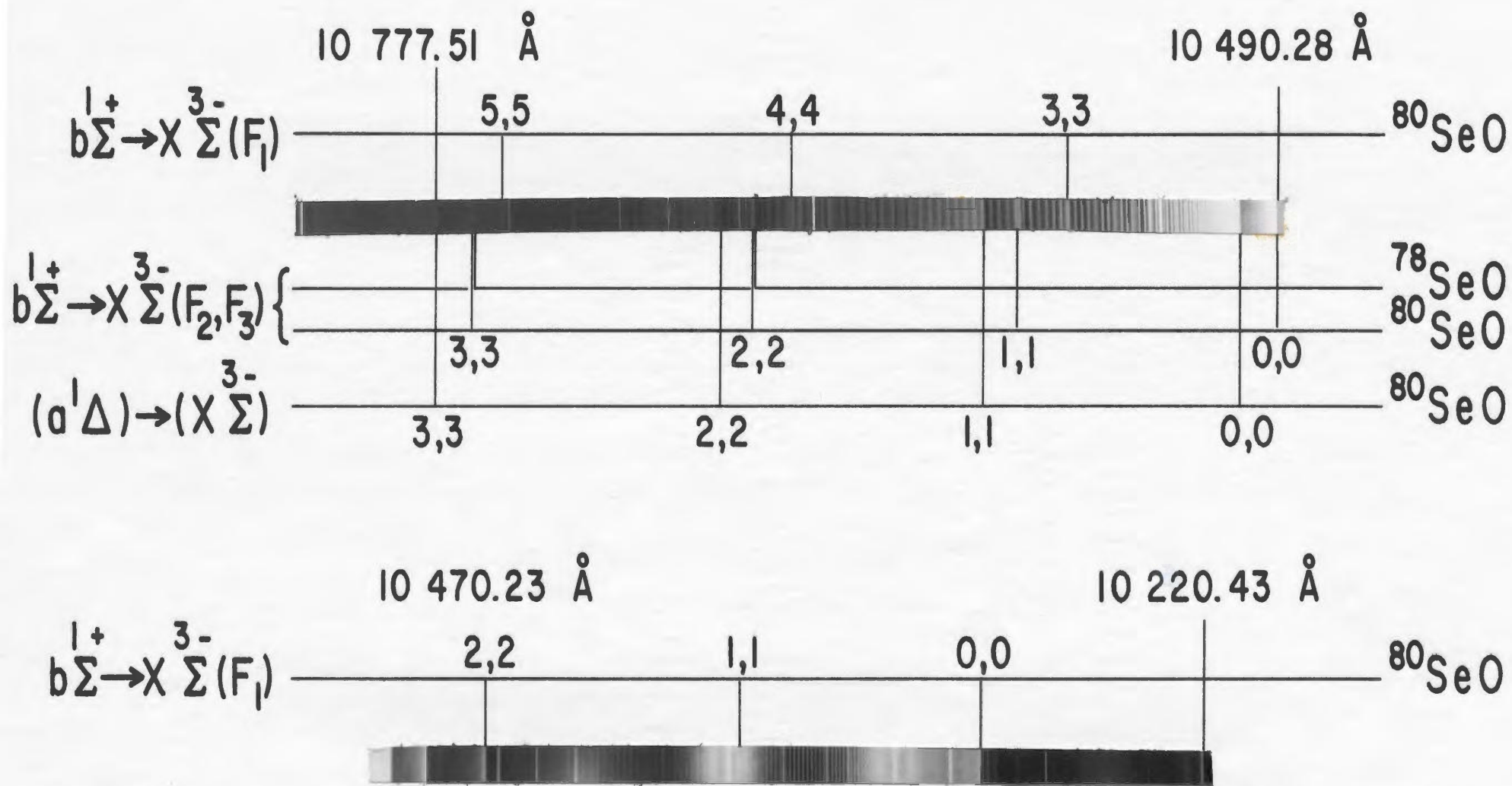
Plate II(a)   The $b\,^1\Sigma^+ \rightarrow X\,^3\Sigma^-$ and $(a\,^1\Delta) \rightarrow (X\,^3\Sigma^-)$ System of SeO in the Region 10 780 - 10 220 Å
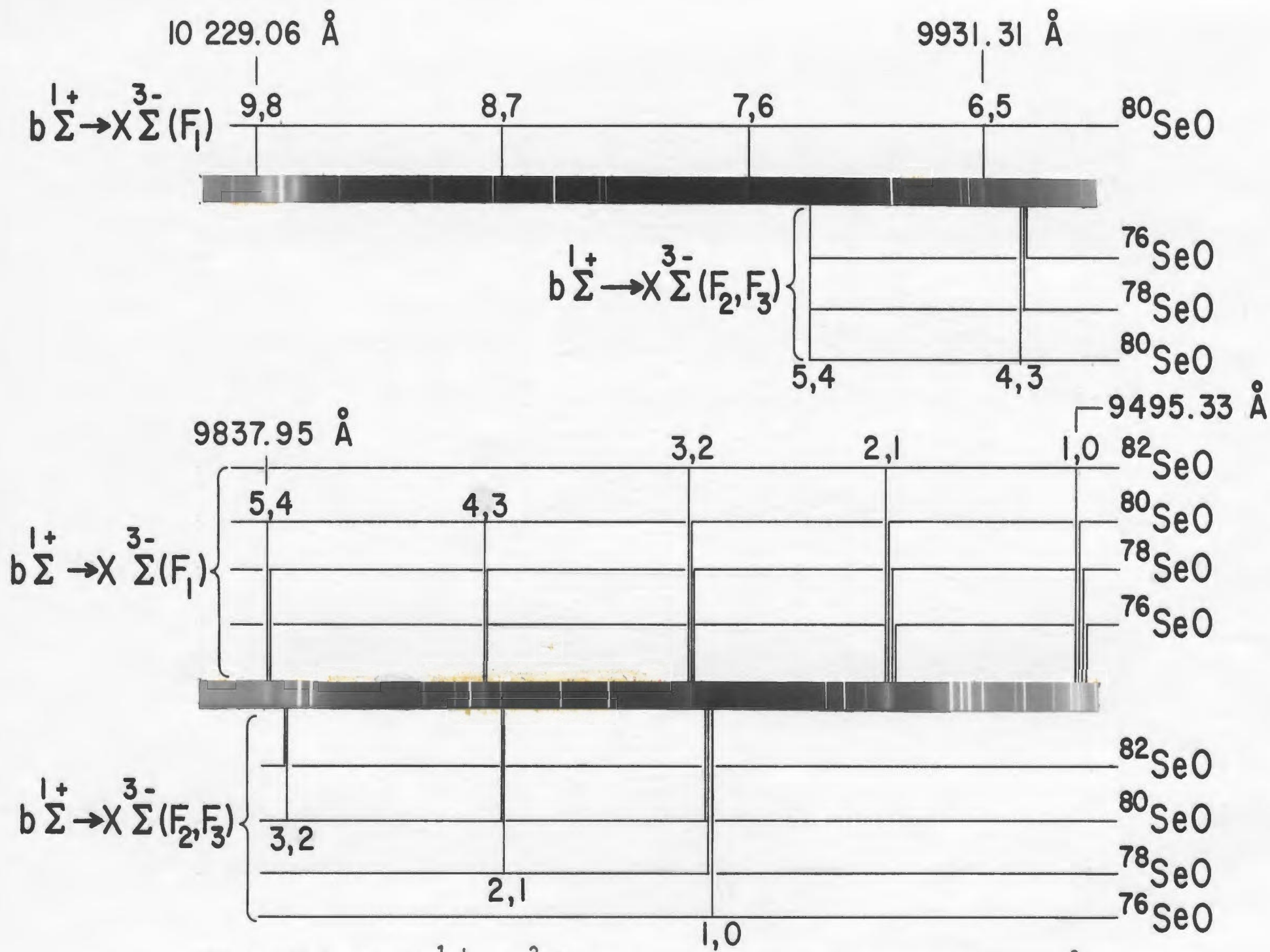
Plate II(b)   The $b\ ^1\Sigma^+ \rightarrow X\ ^3\Sigma^-$ System of SeO in the Region 10 230 - 9490 Å

(a-X) of SeO. It will be shown below that the b - X system
arises most probably from the b $^1\Sigma^+$ - X $^3\Sigma^-$ transition. Barrow
and Deutsch (1963) analyzed the rotational structure of the
B $^3\Sigma^-$ - X $^3\Sigma^-$ system of SeO and found that the term value of
F_1 level with respect to F_2 in the X $^3\Sigma^-$ state is -172 cm^{-1}
which is unusually large (also refer to section 3.3(c)). These
authors also found that the F_2 and F_3 levels of the X $^3\Sigma^-$ state
lie very close together. In the spectrum obtained in the present
investigation (see Plate 11(a)), the separations of the intense
band heads at 10 259.86 Å (9710.0 cm^{-1}), 10 381.74 Å (9629.7 cm^{-1}),
and 10 470.23 Å (9548.3 cm^{-1}), from those at 10 490.28 Å (9530.0 cm^{-1}),
10 580.14 Å (9445.2 cm^{-1}), and 10 670.63 Å (9368.9 cm^{-1}), respectively,
are 180.0 cm^{-1}, 180.6 cm^{-1} and 179.4 cm^{-1}. These suggest that
each of the two groups of bands form a sub-system involving the
ground state $^3\Sigma^-$ of the SeO molecule. The groups of bands discussed
above together with some other bands at longer wavelengths are
identified as the $\Delta v(=v' - v'') = 0$ sequences and the groups of bands
at shorter wavelengths (shown in Plate 11(b)) are assigned to
$\Delta v = +1$ sequences of the two sub-systems. The sub-system with its
0,0 band at 9710.0 cm^{-1} is assigned to be the b $^1\Sigma^+$ - $^3\Sigma^-(F_1)$
transition and the one with its 0,0 band at 9530.0 cm^{-1} is assigned
to the b $^1\Sigma^+$ - X $^3\Sigma^-(F_2,F_3)$ transition. The wavelengths and the
vacuum wavenumbers of the band heads, the visual estimates of their
relative intensities and their vibrational quantum numbers are listed
in Table II. In the b - X system several isotope band heads corresponding

TABLE II

Band Heads of the $b\,^1\Sigma^+ \to X\,^3\Sigma^-$ System [a]

in the Region 10 765 - 9490 Å

λ_{air}(Å)	$\nu_{obs.}$(cm^{-1}) (vacuum)	Intensity [b]	Molecule	v',v"	$\nu_{obs.} - \nu_{calc.}$
		Sub-system $b\,^1\Sigma^+ - X\,^3\Sigma^-(F_1)$			
10 753.49	9296.8	vw	^{80}SeO	5,5	-0.1
10 656.51	9381.4	w	^{80}SeO	4,4	-0.4
10 561.87	9465.4	m	^{80}SeO	3,3	-0.1
10 470.23	9548.3	s	^{80}SeO	2,2	0.0
10 381.74	9629.7	s	^{80}SeO	1,1	+0.4
10 259.86	9710.0	vs	^{80}SeO	0,0	+0.1
10 229.06	9773.4	vw	^{80}SeO	9,8	-2.2
10 127.93	9871.0	vw	^{80}SeO	8,7	-3.1
10 027.75	9969.6	vw	^{80}SeO	7,6	-1.8
9931.31	10 066.4	w	^{80}SeO	6,5	-1.1
9837.95	10 161.9	w	^{80}SeO	5,4	-0.5
9837.09	10 162.8	w	^{78}SeO	5,4	
9747.84	10 255.9	m	^{80}SeO	4,3	+0.2
9746.81	10 257.0	w	^{78}SeO	4,3	
9661.53	10 347.5	w	^{82}SeO	3,2	
9660.42	10 348.7	m	^{80}SeO	3,2	+0.1

TABLE II (Continued)

Band Heads of the b $^1\Sigma^+ \rightarrow$ X $^3\Sigma^-$ System [a]

in the Region 10 765 - 9490 $\overset{o}{A}$

$\lambda_{air}(\overset{o}{A})$	$\nu_{obs.}(cm^{-1})$ (vacuum)	Intensity [b]	Molecule	v',v"	$\nu_{obs.} - \nu_{calc.}$
9659.25	10 349.9	w	^{78}SeO	3,2	
9577.11	10 438.7	w	^{82}SeO	2,1	
9575.80	10 440.1	s	^{80}SeO	2,1	+0.2
9574.45	10 441.6	m	^{78}SeO	2,1	
9573.09	10 443.1	w	^{76}SeO	2,1	
9495.33	10 528.6	w	^{82}SeO	1,0	
9493.83	10 530.3	s	^{80}SeO	1,0	+0.3
9492.16	10 532.1	m	^{78}SeO	1,0	
9490.55	10 533.9	w	^{76}SeO	1,0	

Sub-system b $^1\Sigma^+$ - X $^3\Sigma^-(F_2,F_3)$

10 760.90	9290.4	vw	^{80}SeO	3,3	+0.8
10 759.82	9291.3	vw	^{78}SeO	3,3	
10 670.63	9368.9	w	^{80}SeO	2,2	-0.2
10 669.85	9369.6	w	^{78}SeO	2,2	
10 580.14	9449.1	m	^{80}SeO	1,1	-0.3
10 490.28	9530.0	s	^{80}SeO	0,0	-0.1
10 004.00	9993.3	vw	^{80}SeO	5,4	+2.3

TABLE II (Continued)

Band Heads of the $b\ ^1\Sigma^+ \rightarrow X\ ^3\Sigma^-$ System [a]

in the Region 10 765 - 9490 $\overset{o}{A}$

$\lambda_{air}(\overset{o}{A})$	$\nu_{obs.}(cm^{-1})$ (vacuum)	Intensity [b]	Molecule	v',v"	$\nu_{obs.} - \nu_{calc.}$
9916.74	10 081.2	w	^{80}SeO	4,3	-0.3
9915.72	10 082.2	w	^{78}SeO	4,3	
9914.54	10 083.4	vw	^{76}SeO	4,3	
9830.32	10 169.8	m	^{82}SeO	3,2	
9828.88	10 171.3	m	^{80}SeO	3,2	0.0
9740.88	10 263.2	m	^{80}SeO	2,1	+1.0
9738.88	10 265.3	w	^{78}SeO	2,1	
9656.22	10 353.2	vw	^{80}SeO	1,0	-0.9
9654.29	10 355.3	m	^{78}SeO	1,0	
9632.65	10 357.0	w	^{76}SeO	1,0	

a: All bands are degraded to longer wavelengths.

b: Abbreviations used: vs, s, m, w and vw denote very strong, strong, medium, weak and very weak, respectively.

to ^{82}SeO, ^{78}SeO, ^{76}SeO are also observed in addition to the
main heads of the ^{80}SeO species. The isotope heads are shown
in Plates 11(a) and 11(b) and the data are included in Table II.
More details of the isotope effect will be given below. The
assignment of the vibrational quantum numbers was carried out
by fitting the wave numbers of the band heads of ^{80}SeO in a
Deslandres vibrational scheme which is shown in Table III. Since
only two sequences are observed, the bands fall into a very narrow
Franck - Condon Parabola. Mean values of the vibrational intervals
$\Delta G_{v+\frac{1}{2}}$ obtained from the Deslandres scheme and the second differences
$\Delta^2 G_v$ are summarized in Table IV.

The values of $\Delta G_{v+\frac{1}{2}}$ are plotted against the corresponding
$v+\frac{1}{2}$ values for the lower and upper states of each of the sub-
systems as shown in Fig. 6. These plots give straight lines which
can be expressed as (see Eq. 3-3)

$$(3-8) \qquad G(v) = \omega_e \left(v + \tfrac{1}{2} \right) - \omega_e x_e \left(v + \tfrac{1}{2} \right)^2.$$

The intercepts and slopes of these straight lines which were
determined by a least square method represent $(\omega_e - \omega_e x_e)$ and
$-2 \omega_e x_e$ respectively. The values of ω_e and $\omega_e x_e$ thus
obtained for each sub-system were used to calculate the origin ν_e
from Eq. (3-4) by substituting the calculated values $G'(v')$ and
$G''(v'')$ and the corresponding observed values of the band heads.
In the calculation of the mean values of ν_e for the $b - X \, ^3\Sigma^-(F_1)$
sub-systems the data of 12 sharp bands of ^{80}SeO were used whereas

TABLE III

VIBRATIONAL SCHEME OF THE $b(\Sigma^{1+}) \rightarrow X(\Sigma^{3-})$ SYSTEM OF ^{80}SeO

v' \ v''	0	1	2	3	4	Mean $\Delta G'$ $V + \tfrac{1}{2}$
0	9 710.0(F_1)					
	180.0					
	9 530.0(F_2)					
	820.3					820.3(F_1)
	823.2					823.2(F_2)
1	10 530.3(F_1) 900.6	9 629.7(F_1)				
	177.1	180.6				
	10 353.2(F_2) 904.1	9 449.1(F_2)				
		810.4				810.4(F_1)
		814.1				814.1(F_2)
2		10 440.1(F_1) 891.8	9 548.3(F_1)			
		176.9	179.4			
		10 263.2(F_2) 894.3	9 368.9(F_2)			
			800.4			800.4(F_1)
			802.4			802.4(F_2)
3			10 348.7(F_1) 883.8	9 465.4(F_1)		
			177.4	175.0		
			10 171.3(F_2) 880.9	9 290.4(F_2)		
				790.5		790.5(F_1)
				790.8		790.8(F_2)
4				10 255.9(F_1) 874.5	9 381.4(F_1)	
				174.7		
				10 081.2(F_2)		
Mean $\Delta G''$ $V + \tfrac{1}{2}$	900.6(F_1) 904.1(F_2)	891.8(F_1) 894.3(F_2)	883.3(F_1)) 880.9(F_2)	874.5(F_1)		

TABLE III (Cont'd)

V' \ V''	4	5	6	7	8	Mean $\Delta G'$ $V + \frac{1}{2}$
	780.5					780.5(F_1)
	10 161.9(F_1) 865.1	9 296.8(F_1)				
5	168.6					
	9 993.3(F_2)					
		769.6				769.6(F_1)
6		10 066.4(F_1)				
7			9 969.6(F_1)			
8				9 871.0(F_1)		
9					9 773.4(F_1)	
Mean $\Delta G''$ $V + \frac{1}{2}$		865.1(F_1)				

TABLE IV

Values of Mean $\Delta G_{v+\frac{1}{2}}$ and $\Delta^2 G_v$ of the

b → X System of ^{80}SeO

$v+\frac{1}{2}$	$\Delta G'_{v+\frac{1}{2}}$	$\Delta^2 G'_v$	$\Delta G''_{v+\frac{1}{2}}$	$\Delta^2 G''_v$
		Sub-system b $^1\Sigma^+$ - X $^3\Sigma^-(F_1)$		
0.5	820.3		900.6	
		-9.9		-8.8
1.5	810.4		891.8	
		-10.0		-8.5
2.5	800.4		883.3	
		-9.9		-8.8
3.5	790.5		874.5	
		-10.0		-9.4
4.5	780.5		865.1	
		-11.0		
5.5	769.5			

TABLE IV (Continued)

Values of Mean $\Delta G_{v+\frac{1}{2}}$ and $\Delta^2 G_v$ of the
b → X System of ^{80}SeO

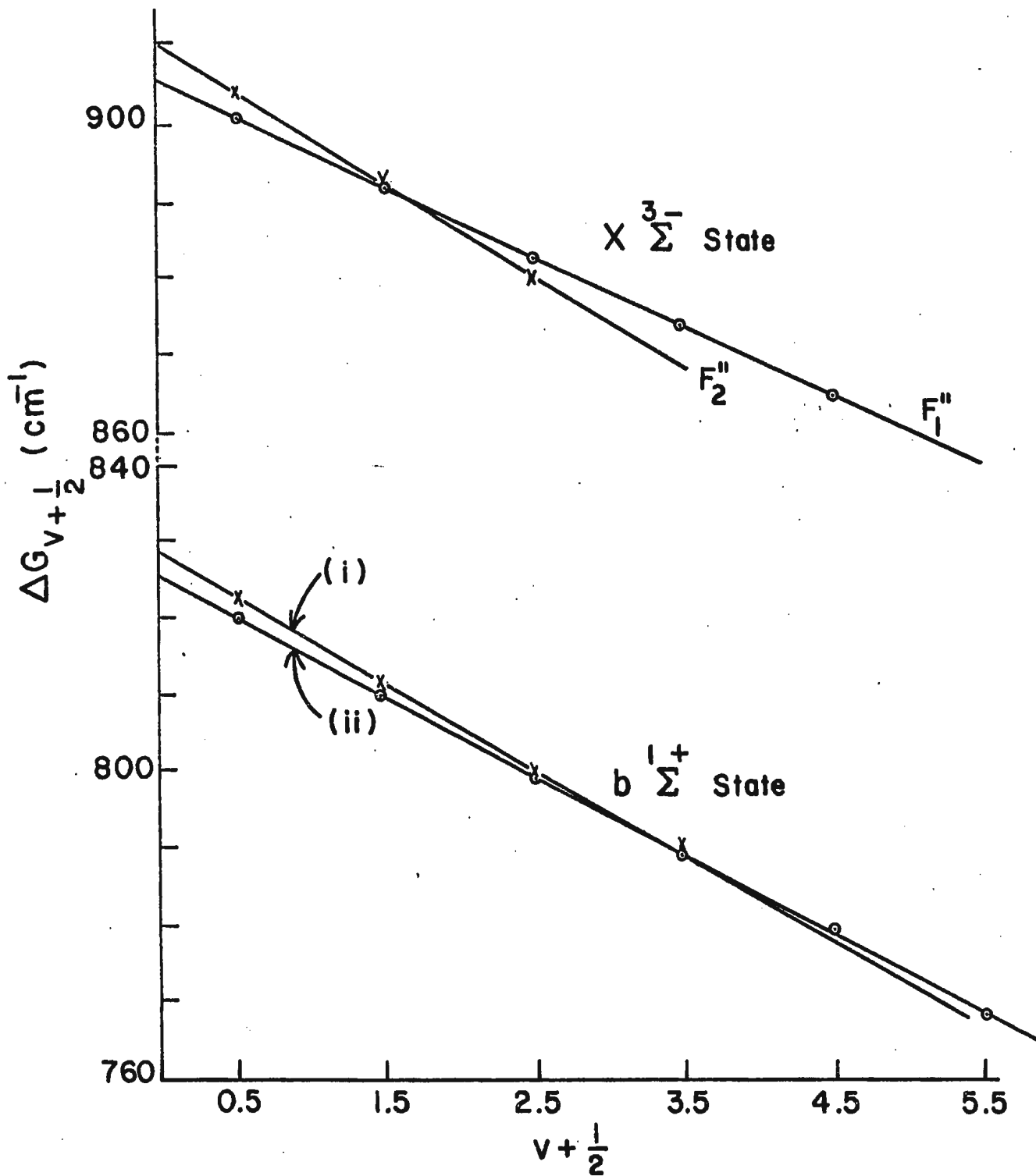| $v+\frac{1}{2}$	$\Delta G'_{v+\frac{1}{2}}$	$\Delta^2 G'_v$	$\Delta G''_{v+\frac{1}{2}}$	$\Delta^2 G''_v$
		Sub-System b $^1\Sigma^+$ - X $^3\Sigma^-$(F$_2$,F$_3$)		
0.5	823.2		904.1	
		-9.1		-9.8
1.5	814.1		894.3	
		-11.7		-13.4
2.5	802.4		880.9	
		-11.6		
3.5	790.8			

Fig. 6. Plots of $\Delta G_{v+\frac{1}{2}}$ vs. $v+\frac{1}{2}$ For the $X^3\Sigma^-$ and $b^1\Sigma^+$ States of SeO . For the $b^1\Sigma^+$ State , Straight Lines (i) and (ii) Are Drawn From the $G_{v+\frac{1}{2}}$ Values Obtained From the Analyses of $b - X(F_1) -$ and $b - X(F_2, F_3) -$ Sub-systems, Respectively .

for the $b - X {}^3\Sigma^-(F_2, F_3)$ sub-system the data of 6 sharp bands were used. The mean values of ν_e for these two sub-systems are 9749.0 ± 0.4 cm^{-1} and 9570.7 ± 0.4 cm^{-1} respectively. Finally the wave numbers of the band heads of the two systems are represented by the following equations (see Eq. (3-4)):

For the $b {}^1\Sigma^+ - X {}^3\Sigma^-(F_1)$ sub-system of ^{80}SeO:

$$(3-9) \quad \nu = 9749.0 + 830.6 \, (v' + \tfrac{1}{2})^2 - 5.0 \, (v' + \tfrac{1}{2})^2$$
$$- \{909.5 \, (v'' + \tfrac{1}{2}) - 4.4 \, (v'' + \tfrac{1}{2})^2\}.$$

For the $b {}^1\Sigma^+ - X {}^3\Sigma^-(F_2, F_3)$ sub-system of ^{80}SeO:

$$(3-10) \quad \nu = 9570.7 + 834.9 \, (v' + \tfrac{1}{2}) - 5.5 \, (v' + \tfrac{1}{2})^2$$
$$- \{916.3 \, (v'' + \tfrac{1}{2}) - 5.8 \, (v'' + \tfrac{1}{2})^2\}.$$

The wavenumbers of the band heads of ^{80}SeO were calculated by means of Eqs. (3-9) and (3-10) and the differences $\nu_{obs.} - \nu_{calc.}$ are given in the last column of Table II. These differences range from 0.0 to 0.5 cm^{-1} for the sharp bands and from 1.1 to 3.1 cm^{-1} for the diffuse bands.

The ground state vibrational constants obtained in the present work are in good agreement with those obtained from the analysis of the $B {}^3\Sigma^- - X {}^3\Sigma^-$ system of ^{80}SeO by Barrow and Deutsch, (1963), namely, $\omega_e = 914.69$ cm^{-1} and $\omega_e x_e = 4.52$ cm^{-1} for the F_1 state and $\omega_e = 915.43$ cm^{-1} and $\omega_e x_e = 4.52$ cm^{-1} for the F_2, F_3 states. The small discrepancies between our values and those of Barrow and Deutsch (1963) can be attributed to the fact that the

latter derived the vibrational constants from the band origins while we used the band head data in the present analysis. The difference in the system origins in this analysis is -178.3 cm^{-1} which compares favourably with the T_{oo} value -172 cm^{-1} between the F_2 and F_1 levels obtained by Barrow and Deutsch (1963). Thus it is concluded that the lower state of the b - X system is the ground state $X \, ^3\Sigma^-$.

(b) Isotope Effect:

Several of $^1\Sigma - F_1$ as well as $^1\Sigma - F_2, F_3$ sub-bands of ^{82}SeO, ^{80}SeO, ^{78}SeO and ^{76}SeO are clearly resolved. The reduced mass μ , the factor $\rho = (\mu/\mu(^{80}\text{SeO}))^{\frac{1}{2}}$ and the relative abundances of these isotopes are listed below:

Isotope	μ(a.m.u.)	ρ	Relative Abundance (%)
^{80}SeO	13.328	1.000	49.9
^{82}SeO	13.382	1.002	9.0
^{78}SeO	13.271	0.998	23.6
^{76}SeO	13.212	0.996	9.1

The values of the shifts of the band heads of ^{76}SeO, ^{78}SeO and ^{82}SeO from the corresponding band heads of ^{80}SeO were calculated from Eq. (3-7) using the vibrational constants for ^{80}SeO. The observed and calculated isotope shifts are given in Table V. It is seen that

TABLE V

Isotopic Shifts (in cm^{-1})

v',v''	$\Delta\nu(^{80}SeO - ^{76}SeO)$		$\Delta\nu(^{80}SeO - ^{78}SeO)$		$\Delta\nu(^{80}SeO - ^{82}SeO)$	
	obs.	calc.	obs.	calc.	obs.	calc.
Sub-system b $^1\Sigma^+$ - X $^3\Sigma^-(F_1)$						
1,0	-3.6	-3.3	-1.8	-1.6	+1.7	+1.6
2,1	-3.0	-2.9	-1.5	-1.4	+1.4	+1.4
3,2	-	-2.5	-1.2	-1.2	+1.2	+1.2
4,3	-	-2.0	-1.1	-1.0	-	+0.9
5,4	-	-1.6	-0.9	-0.7	-	+0.7

TABLE V (Continued)

Isotopic Shifts (in cm^{-1})

v',v"	$\Delta\nu(^{80}SeO - {}^{76}SeO)$		$\Delta\nu(^{80}SeO - {}^{78}SeO)$		$\Delta\nu(^{80}SeO - {}^{82}SeO)$	
	obs.	calc.	obs.	calc.	obs.	calc.
	Sub-System b $^1\Sigma^+$ - X $^3\Sigma^-(F_2,F_3)$					
1,0	-3.8	-3.3	-2.1	-1.6	-	+1.6
2,1	-	-2.9	-2.1	-1.4	-	+1.4
3,2	-	-2.5	-	-1.2	+1.5	+1.2
4,3	-2.2	-2.0	-1.0	-1.0	-	+0.9
0,0	-	-0.2	-	-0.1	-	+0.1
1,1	-	-0.5	-	-0.3	-	+0.3
2,2	-	-0.9	-0.7	-0.6	-	+0.4
3,3	-	-1.3	-0.9	-0.9	-	+0.6

the agreement between them is excellent, which proves that the vibrational numbering of the bands is essentially correct.

(c) Observed Vibrational Structure:

The observed vibrational structure of the bands of the b - X system can be explained on the basis of a $^1\Sigma^+$ - $^3\Sigma^-$ transition. According to Schlapp (1932) (see Herzberg, 1950, P. 223) the term values of the three triplet components of a $^3\Sigma$ state (spin S = 1, multiplicity = 2S + 1 = 3) are given by

$$(3\text{-}11) \quad F_1(N) = B_v N(N + 1) - D_v N^2 (N + 1)^2 + (2N + 3) B_v - \lambda_v$$
$$- \{(2N + 3)^2 B_v^2 + \lambda_v^2 - 2\lambda_v B_v\}^{\frac{1}{2}} + \gamma_v (N + 1) ,$$

$$(3\text{-}12) \quad F_2(N) = B_v N(N + 1) - D_v N^2 (N + 1)^2 ,$$

$$(3\text{-}13) \quad F_3(N) = B_v N(N + 1) - D_v N^2 (N + 1)^2 - (2N - 1) B_v - \lambda_v$$
$$+ \{(2N - 1)^2 B_v^2 + \lambda_v^2 - 2\lambda_v B_v\}^{\frac{1}{2}} - \gamma_v N .$$

Here F_1, F_2 and F_3 refer to the levels with J = N + 1, N and N - 1 respectively, and J is the quantum number of the total angular momentum and N is the quantum number representing the angular momentum apart from the spin of the electrons (Note: J = N + S, N + S - 1, ... |N - S|). B_v is the rotational constant, D_v is the stretching constant, and λ_v and γ_v are respectively the spin - spin and spin - rotation interaction constants.

The transition $^1\Sigma$ - $^3\Sigma$ is forbidden because of the approximate selection rule $\Delta S = 0$ which is based on the assumption

of zero spin - orbit interaction (Herzberg 1950, 1968). The branches expected to result from a $^1\Sigma^+ - ^3\Sigma^-$ transition are shown in Fig. 7. Considering the electric dipole selection rules ($+ \leftrightarrow -$; $\Delta J = 0$, ± 1), five branches are expected, namely, three branches of Q form ($\Delta N = 0$) ^QQ, ^QP and ^QR and one branch each of S ($\Delta N = +2$) and O ($\Delta N = -2$) forms ^SR and ^OP (see Herzberg and Hugo, 1955). The selection rule that Σ^- states do not combine with Σ^+ states does not apply to intercombination systems such as $^1\Sigma^+ - ^3\Sigma^-$ as was shown by Schlapp (1932). In Fig. 8, we represent all the expected five branches for the b $^1\Sigma^+ - $ X $^3\Sigma^-$ transition of SeO. The term values for the X $^3\Sigma^-$ v" = 0 state in Fig. 8 were calculated from Eqs. (3-11), (3-12) and (3-13) using the following constants obtained by Barrow and Deutsch (1963): B_0'' (F_1) = 0.4638 cm^{-1}, B_0'' (F_2) = 0.4688 cm^{-1}, B_0'' (F_3) = 0.4645 cm^{-1}, λ" = 86.4 cm^{-1} (γ is negligibly small). The large value of λ of the $^3\Sigma^-$ state of SeO makes the structure of its b $^1\Sigma^+ - $ X $^3\Sigma^-$ system somewhat different from the corresponding systems of the analogous molecules O_2, SO, etc. It is to be noted that the values of λ for O_2 and SO are only 1.985 cm^{-1} (Townes and Schalow, 1955) and 5.2789 cm^{-1} (Amano et al 1967) respectively. If λ is small (for example, for the X $^3\Sigma^-$ state of NF, λ = 1.21 cm^{-1} (Douglas and Jones, 1966)), for each N value, except for the first two or three, the F_1 and F_3 levels will be close together with F_2 levels separated from them by an amount approximately equal to λ . However, when λ is very large as in
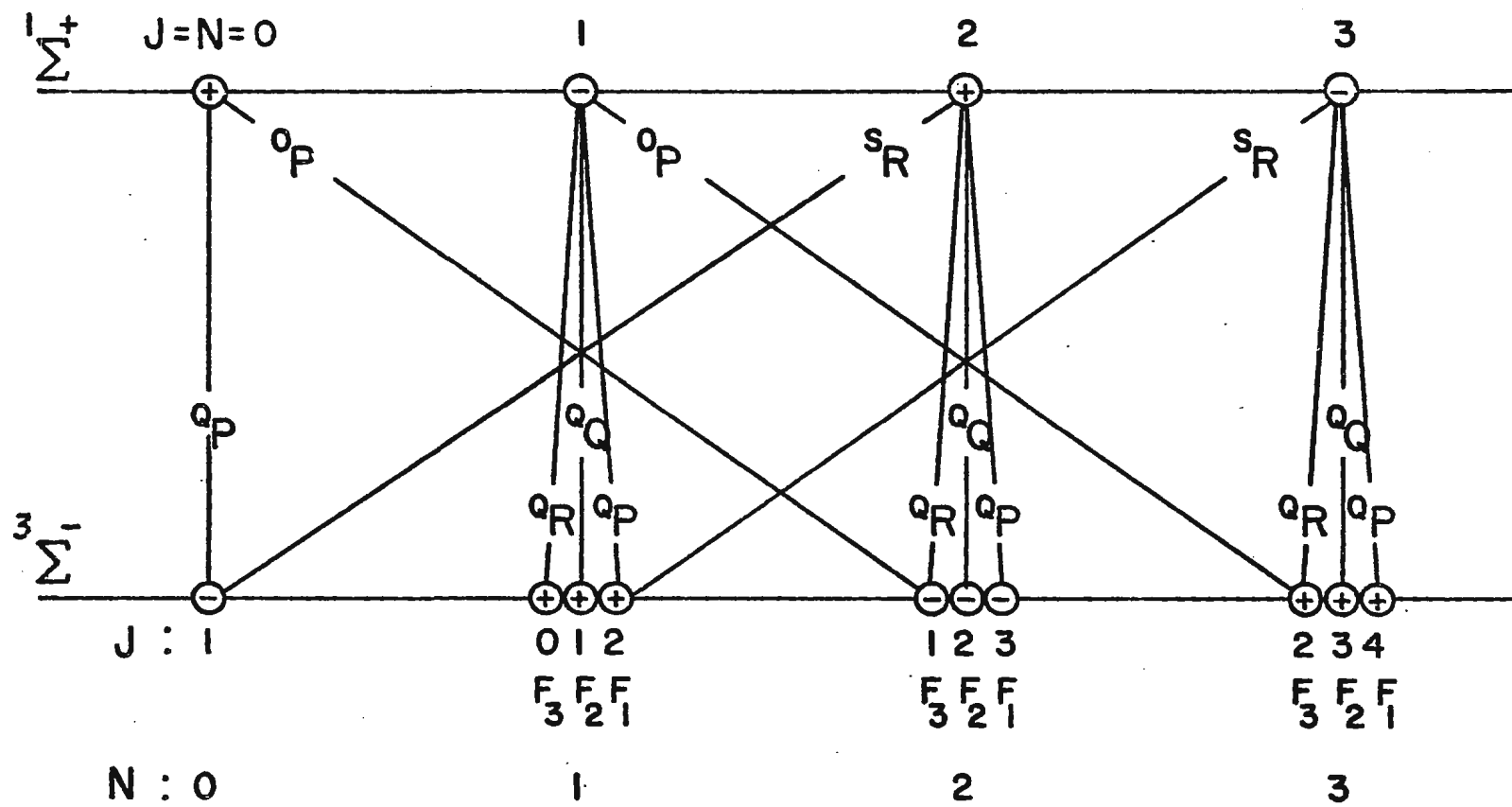
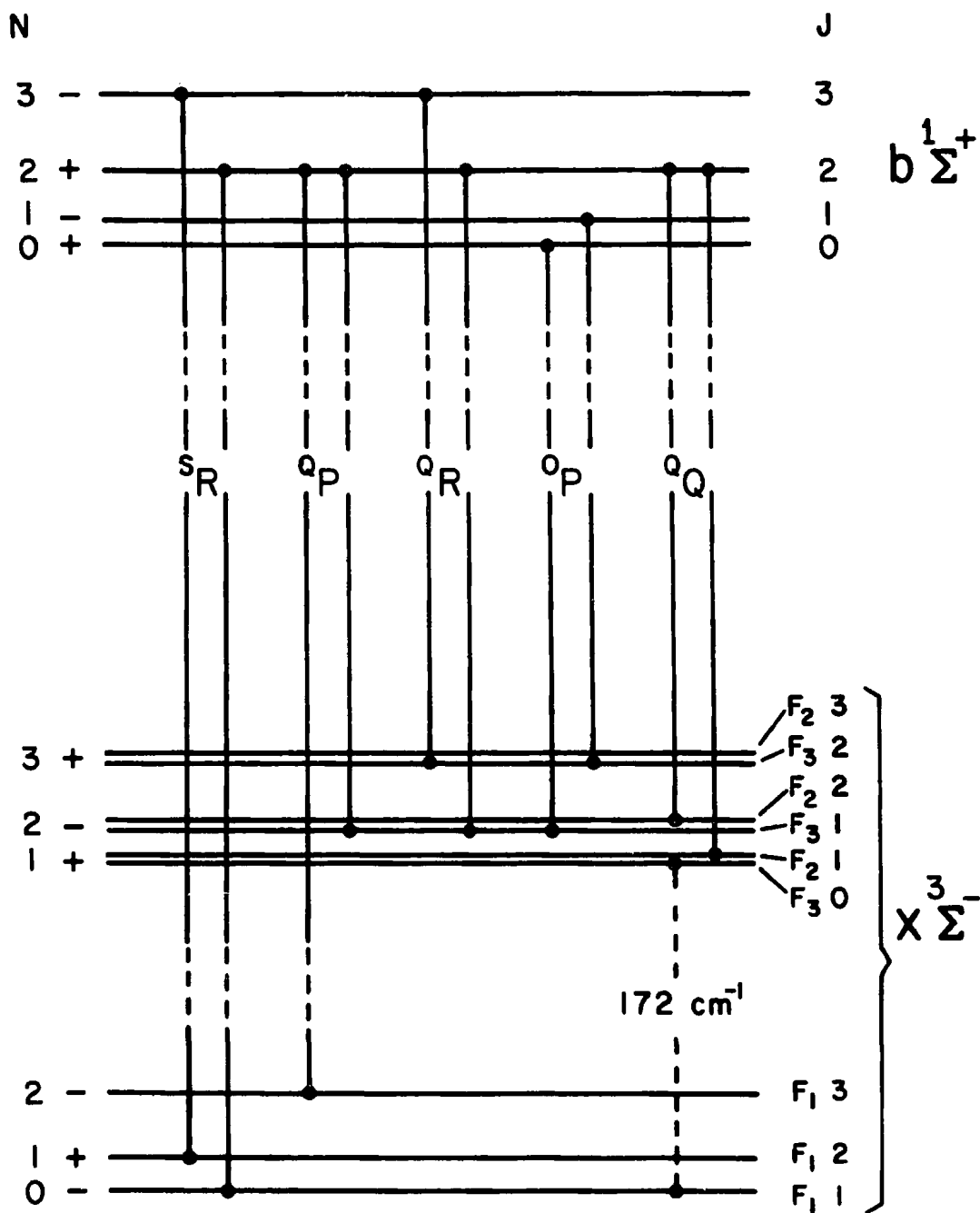Fig. 7. Origin of the Branches of a Band in a $^1\Sigma^+$ - $^3\Sigma^-$ Transition .

Fig. 8 Energy Level Diagram for a $^1\Sigma^+$ - $^3\Sigma^-$ Band, with $^3\Sigma^-$ State Having a Large Value of the Spin Splitting Constant λ.

the case of the $X\ ^3\Sigma^-$ state of SeO, for each value of N

F_2 and F_3 levels will be very close together with F_1 level separated from them by an amount equal to $\sim 2\lambda$. Since the ^SR and ^QP branches arise from the $\Sigma^+ - F_1$ sub-system (See Fig. 8), the band heads observed for the $b\ ^1\Sigma^+ - X\ ^3\Sigma^-(F_1)$ sub-system of SeO could be ^SR or ^QP. Also, since ^QR, ^OP and ^QQ branches arise for a $^1\Sigma^+ - F_2$, F_3 sub-system (See Fig. 8), the band heads observed for the $b\ ^1\Sigma^+ - X\ ^3\Sigma^-(F_2, F_3)$ of SeO could be formed by one of these three branches.

3.4 The a - X System of SeO:

Four bands degraded to longer wavelengths in the region 10 750 - 10 500 $\overset{o}{A}$ (Plate 11(a)) could not be fitted into the b - X system. These bands seem to form the $\Delta v = 0$ sequence of a new band system which is tentatively assigned to a $^1\Delta - X\ ^3\Sigma^-$ transition of SeO (See Section 3.5). The wavelengths, vacuum wavenumbers, visual estimates of the relative intensities and tentative vibrational assignments are given in Table VI. No vibrational constants can be derived for this system.

3.5 Discussion:

The transitions assigned for the two systems discussed above should of course be confirmed by a detailed rotational analysis of these band systems. The electron configurations of the SeO molecule are discussed in Section 4.6(b) in Chapter 4.

TABLE VI

Band Heads of the $(a^1\Delta) - (X^3\Sigma^-)$ System in the Region 10 780 - 10 500 Å *

λ_{air} (Å)	ν_{vac} (cm^{-1})	Intensity	v', v"
10 777.51	9276.0	vw	3,3
10 684.50	9356.8	w	2,2
10 591.30	9439.1	s	1,1
10 503.05	9518.4	vs	0,0

* The notation for the intensities is the same as the one given in Table II.

CHAPTER 4

THE FAR ULTRAVIOLET EMISSION SPECTRUM OF SeO

4.1 Introduction:

As reported in Section 1.2, the far ultraviolet emission

spectrum of SeO was first observed by Haranath (1964) under the

low dispersion (17.3 $\overset{o}{A}$/mm) of a 1 m normal incidence vacuum

grating spectrograph. In the present work the emission spectrum

of SeO in the region 2480 - 1930 $\overset{o}{A}$ was photographed on Kodak SWR

plates in the first and third orders of a 2 m Bausch and Lomb

grating spectrograph at dispersions of 4.13 $\overset{o}{A}$/mm and 1.29 $\overset{o}{A}$/mm

respectively at 2100 $\overset{o}{A}$. Copper arc lines were used as wavelength

standards. All the experimental details are described in detail

in Chapter 2. The general appearance of the bands which are all

degraded to shorter wavelengths is shown in the first order contact

spectrogram in Plate III. The bands have been re-analyzed into five

band systems which are designated as $c(^1\Sigma+) - b(^1\Sigma+)$, $x_2 - x_1$,

$y_2 - y_1$, $C(^3\Pi) - X\,^3\Sigma^-$ and $D(^3\Sigma^-) - X\,^3\Sigma$, beginning at the longer

wavelength end. The results of the vibrational analyses of these

band systems constitute the rest of this chapter.

4.2 The c - b System:

Nine single-headed bands degraded to shorter wavelengths

in the spectral region 2480 - 2240 $\overset{o}{A}$ have been assigned to the

c - b system and the first order grating spectrogram of these bands

is shown in Plate IV. In the spectrum photographed also in the third

2492.146 Å

1912.891 Å

Cu arc

$c\,{}^{1}\Sigma^{+} \rightarrow b\,{}^{1}\Sigma^{+}$

$x_2 \rightarrow x_1$

$y_2 \rightarrow y_1$

$C\,({}^{3}\Pi) \rightarrow X\,{}^{3}\Sigma^{-}$

$D\,({}^{3}\Sigma^{-}) \rightarrow X\,{}^{3}\Sigma^{-}$

-52-
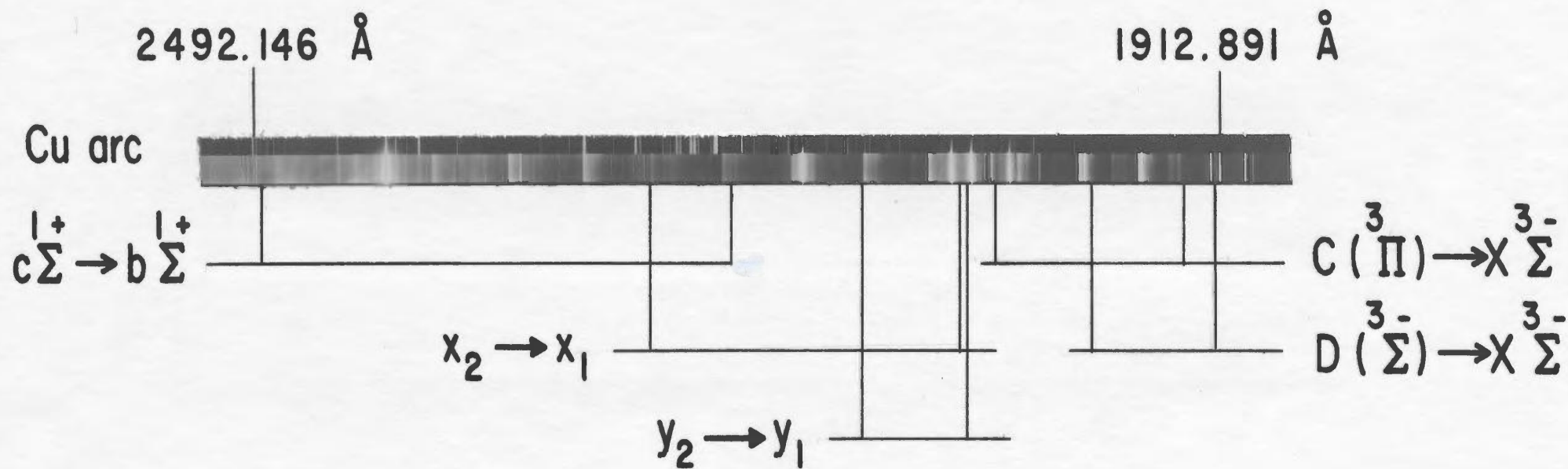
Plate III The Emission Spectrum of SeO in the Region 2490 - 1930 Å:

First Order Contact Spectrogram.

2492.146 Å   2210.267 Å

Cu arc

-53-

0,4   0,3   0,2   0,1   0,0 1,1   1,0 2,1   2,0
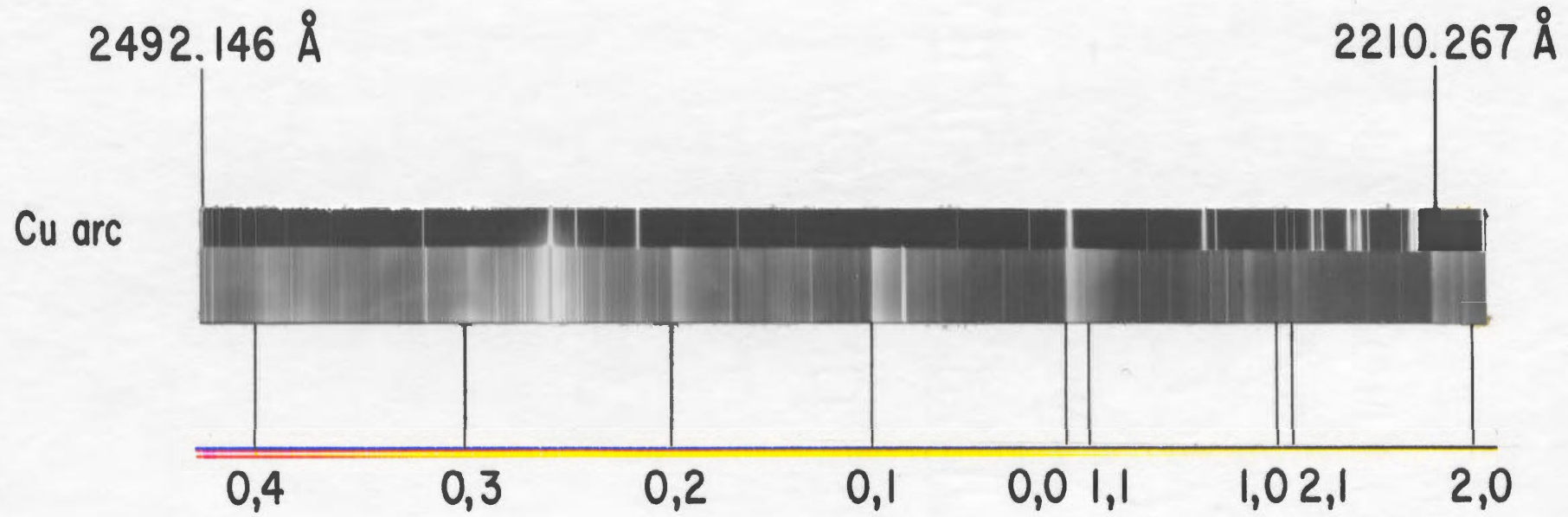
Plate IV The c $^1\Sigma^+$ → b $^1\Sigma^-$ System of SeO.

First Order Grating Spectrogram.

order of the grating (not shown here) the bands remain essentially
single-headed. The wavelengths and the vacuum wavenumbers of the
band heads, the visual estimates of their intensities and their
vibrational quantum numbers are listed in Table VII. The
vibrational quantum numbers assigned to the bands were determined
by fitting the wavenumbers of the band heads in a Deslandres
vibrational scheme which is shown in Table VIII. The values of
$\Delta G_{v+\frac{1}{2}}$ were plotted against $v+\frac{1}{2}$ in Fig. 9. The values of ω_e
and $\omega_e x_e$ were calculated from the intercept ($=\omega_e - \omega_e x_e$) and
slope ($= -2 \omega_e x_e$) of the straight line which were obtained by a
least squares method (Eq. (3-8)). The system origin ν_e was
calculated using the data of all the nine band heads in the same man-
ner as described for the b - X system in Chapter 3. The mean
value of ν_e is 43509 ± 1 cm^{-1}. The wavenumbers ν of the band
heads of the c - b system (See Eq. 3-4) can be represented by the
following formula:

(4-1) $\nu = 43509 + 954 (v' + \frac{1}{2}) - 13.0 (v' + \frac{1}{2})^2$

$- \{840 (v'' + \frac{1}{2}) - 5.5 (v'' + \frac{1}{2})^2\}.$

The wavenumbers of the band heads were calculated by means of
Eq. (4-1). The last column of Table VII gives the differences
$\nu_{obs.} - \nu_{calc.}$ which are less than 3 cm^{-1}. Since the lower state
vibrational frequency (840 cm^{-1}) of the c - b system is in
reasonable agreement with that (835 cm^{-1}) of the b - X system
(Chapter 3), it is concluded that the upper state of the b - X system

TABLE VII

Band Heads of the c → b System [a] in the

Region 2480 - 2200 Å

λ_{air}(Å)	ν_{vac}(cm^{-1})	Intensity [b]	v',v"	$\nu_{obs.} - \nu_{calc.}$ (cm^{-1})
2479.76	40314	vw	0,4	0
2431.68	41111	w	0,3	+1
2384.91	41918	m	0,2	+1
2339.26	42735	s	0,1	+1
2294.81	43563	vs	0,0	-1
2289.68	43661	m	1,1	-2
2246.87	44493	m	1,0	+1
2243.35	44562	m	2,1	-3
2202.15	45396	m	2,0	+2

a: All bands are degraded to shorter wavelengths.

b: See footnote of Table II for abbreviations used.

TABLE VIII

Vibrational Scheme of the c → b System

v' \ v''	0		1		2		3		4	Mean $\Delta G'_{v+\frac{1}{2}}$
0	43563	828	42735	817	41918	807	41111	797	40314	
	930		926							928
1	44493	832	43661							
	903		901							902
2	45396	834	44562							
Mean $\Delta G''_{v+\frac{1}{2}}$		831		817		807		797		
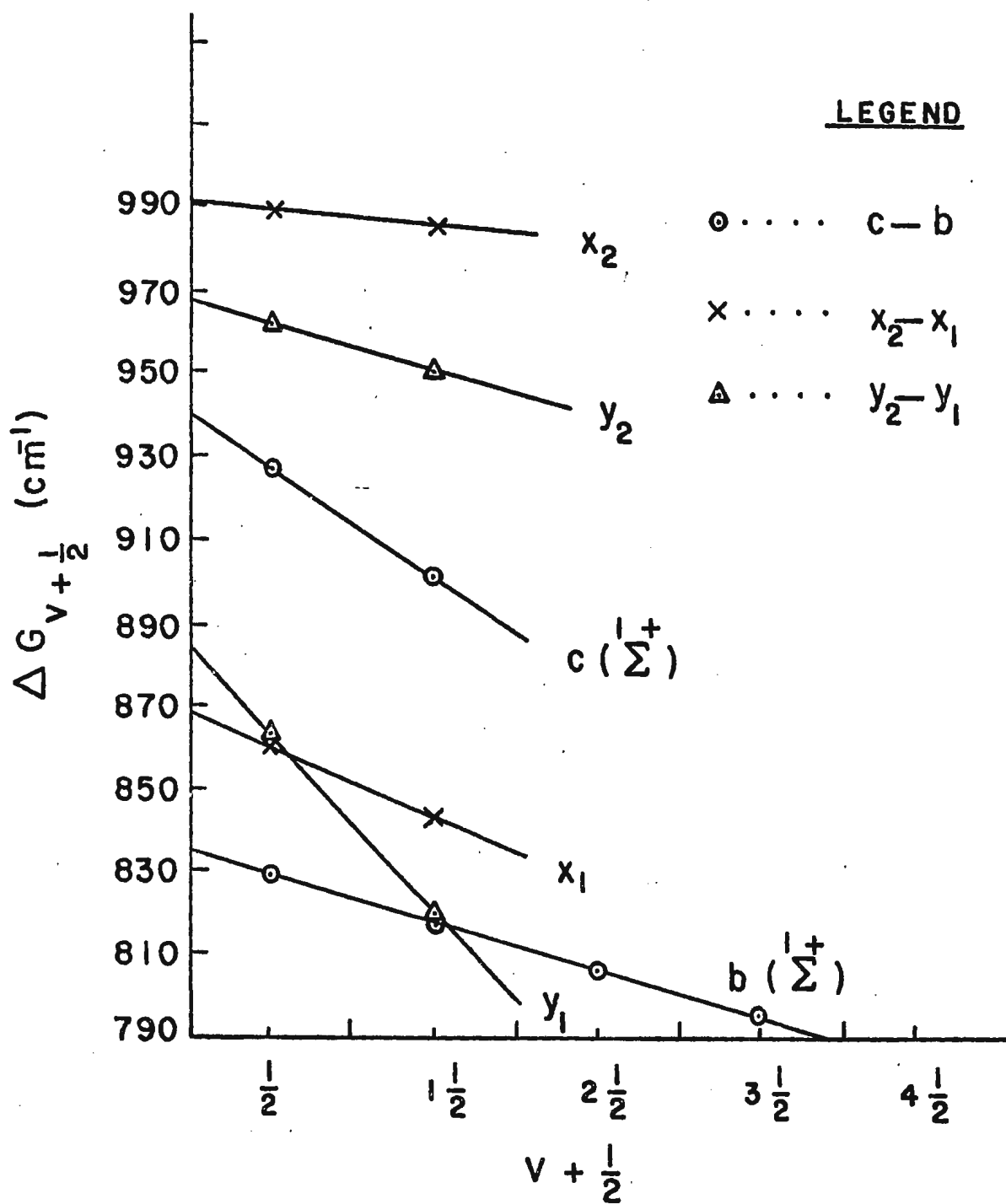
Fig. 9. Plots of $\Delta G_{v+\frac{1}{2}}$ vs. $v+\frac{1}{2}$ For States c, b, x_2, x_1, y_2 and y_1.

is the lower state of the c - b system. From the single-headed nature of the bands it is suggested that tentative transition of the c - b system is $^1\Sigma^+ - ^1\Sigma^+$. However, a confirmation of this must come from a detailed rotational analysis of this band system.

4.3 Two Brief Systems $x_2 - x_1$ and $y_2 - y_1$ in the Region 2255 - 2080 Å:

Two brief systems $x_2 - x_1$ and $y_2 - y_1$ of SeO occur in the region 2250 - 2080 Å. The $x_2 - x_1$ system consists of 7 bands in the region 2250 - 2080 Å and the $y_2 - y_1$ system consists of 5 bands in the region 2130 - 2080 Å. The spectrograms of these two systems obtained from the plates taken in the third order of the grating spectrograph are shown in Plate V. The wavelengths, vacuum wavenumbers and visual estimates of intensities of the bands of these systems are listed in Table IX. The vibrational schemes are presented in Tables X and XI for systems $x_2 - x_1$ and $y_2 - y_1$ respectively. The plots of $\Delta G_{v+\frac{1}{2}}$ against $v+\frac{1}{2}$ are shown in Fig. 9. The values of ω_e and $\omega_e x_e$ for the lower and upper states and of ν_e were determined in the usual manner. The band heads of the two systems are represented by the following formulae:

System $x_2 - x_1$:

$$(4\text{-}2) \quad \nu = 46009 + 993 \ (v' + \tfrac{1}{2}) - 2.0 \ (v' + \tfrac{1}{2})^2$$
$$- \{877 \ (v'' + \tfrac{1}{2}) - 8.0 \ (v' + \tfrac{1}{2})^2\} \ .$$
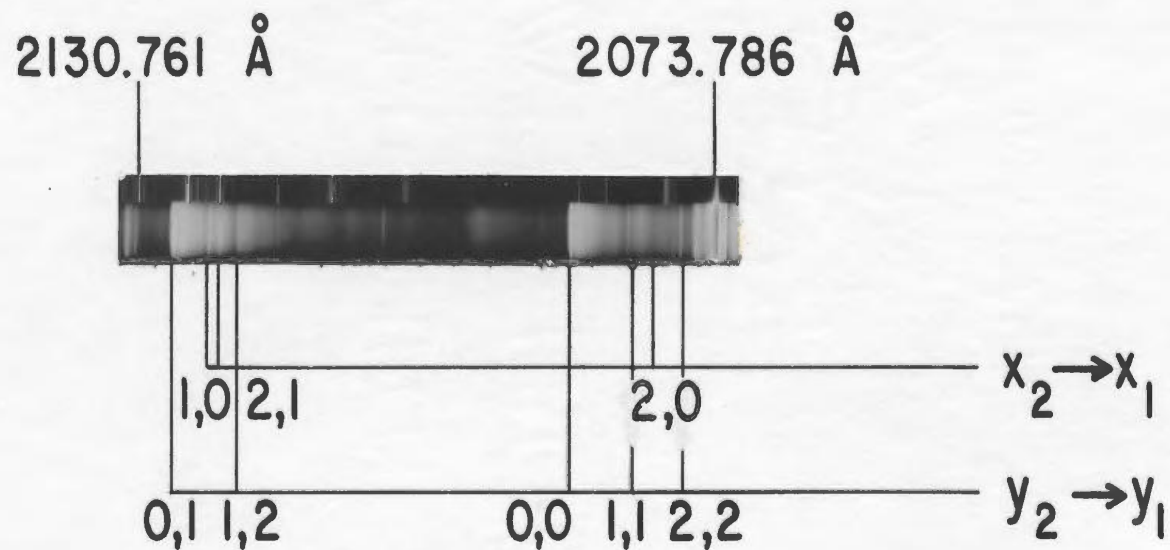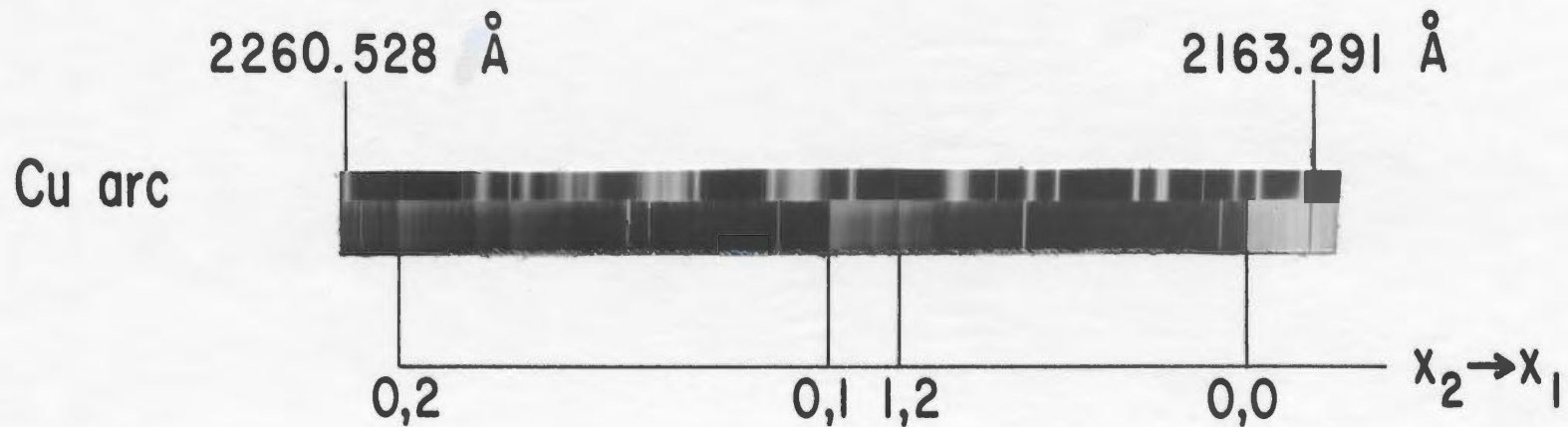
Plate V. The $x_2 \rightarrow x_1$ and $y_2 \rightarrow y_1$ Systems of SeO. Third Order Grating Spectrograms.

TABLE IX

Band Heads of Two Brief Systems [a] in the Region 2255 - 2080 Å

λ_{air}(Å)	$\nu_{vac.}$(cm^{-1})	Intensity [b]	v',v"	$\nu_{obs.} - \nu_{calc.}$ (cm^{-1})
		System $x_2 \rightarrow x_1$		
2253.40	44364	m	0,2	0
2211.29	45208	s	0,1	0
2204.28	45352	m	1,2	-2
2170.03	46068	s	0,0	0
2124.34	47059	m	1,0	+1
2118.71	47184	vw	2,1	+1
2081.27	48045	vw	2,0	+1
		System $y_2 \rightarrow y_1$		
2126.81	47004	vs	0,1	0
2120.44	47145	s	1,2	0
2088.42	47868	vs	0,0	0
2084.09	47967	m	1,1	0
2078.47	48097	w	2,2	0

a: All bands are degraded to shorter wavelengths.

b: See footnote of Table II for abbreviations used.

TABLE X

Vibrational Scheme of the $x_2 \to x_1$ System

$v' \backslash v''$	0		1		2	Mean $\Delta G'_{v+\frac{1}{2}}$
0	46068	860	45208	844	44364	
	991				988	989.5
1	47059				45352	
	986					986.0
2	48045	861	47184			
Mean $\Delta G''_{v+\frac{1}{2}}$		860.5		844		

TABLE XI

Vibrational Scheme of the $y_2 \rightarrow y_1$ System

v' \ v''	0	1	2	Mean $\Delta G'_{v+\frac{1}{2}}$
0	47868 864 47004			
		963		963
1		47967 822 47145		
			952	952
2			48097	
Mean $\Delta G''_{v+\frac{1}{2}}$		864	822	

System $y_2 - y_1$:

(4-3) $\quad \nu = 47830 + 974 (v' + \frac{1}{2}) - 6.0 (v' + \frac{1}{2})^2$

$\qquad\qquad - \{906 (v'' + \frac{1}{2}) - 21.0 (v'' + \frac{1}{2})^2\}$.

The values of $\nu_{obs.} - \nu_{calc.}$ are given in the last column of Table IX. The apparent very small differences between the observed and calculated frequencies is largely due to limited band head data. None of the states x_1, x_2, y_1 and y_2 is found to combine with the other known electronic states of SeO.

4.4 The C - X System:

The C - X system of SeO consists of 8 bands forming the three sequences $\Delta v = -2$, -1 and 0 in the region 2035 - 1950 $\overset{o}{A}$. The third order grating spectrum of this system is reproduced in Plate VI. The data on wavelengths, vacuum wavenumbers, visual estimates of intensities and vibrational assignments of the band heads of this system are given in Table XII. The vibrational scheme of the band heads is presented in Table XIII. Plots of $\Delta G_{v+\frac{1}{2}}$ against $v+\frac{1}{2}$ for the upper and lower states were shown in Fig. 10. The molecular constants of the system were determined as discussed earlier for other systems. The wavenumbers of the band heads are finally represented by the formula,

(4-4) $\quad \nu = 50874 + 1034 (v' + \frac{1}{2}) - 9.3 (v' + \frac{1}{2})^2$

$\qquad\qquad - \{927 (v'' + \frac{1}{2}) - 9.0 (v'' + \frac{1}{2})^2\}$.

2037.132 Å   1921.956 Å

Cu arc

C → X

0,2 1,3   0,1 1,2   0,0 1,1 2,2 3,3

$D\,^3\Sigma(F_1) \rightarrow X\,^3\Sigma(F_1)$

0,1 1,2 2,3   0,0 1,1 2,2

$D\,^3\Sigma(F_2,F_3) \rightarrow X\,^3\Sigma(F_2,F_3)$

0,1 1,2 2,3 3,4   0,0 1,1 2,2 3,3
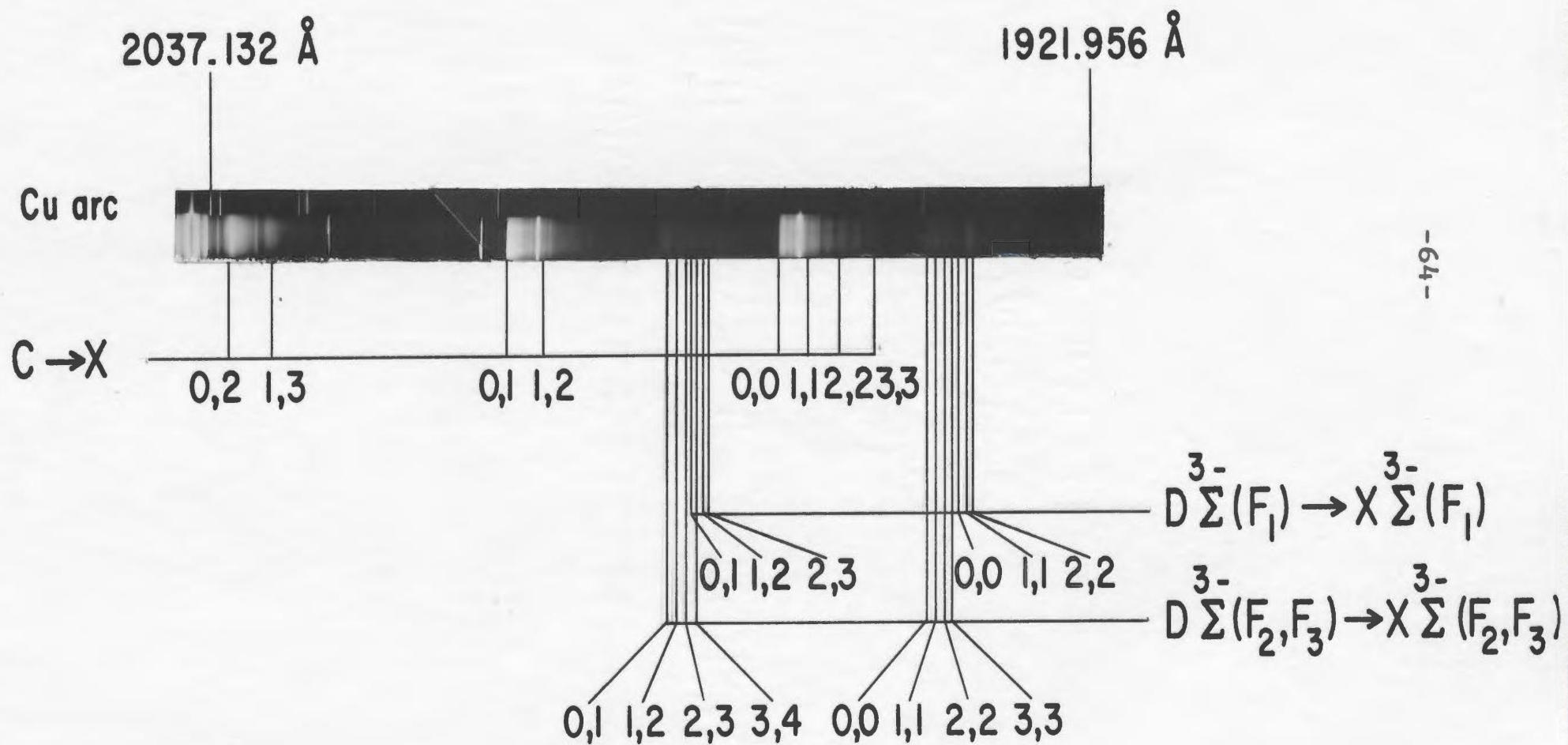
Plate VI   The   C → X   and   D → X   Systems of SeO.   Third Order Grating

Spectrogram.

TABLE XII

Band Heads of the $C \rightarrow X$ System [a] in the

Region 2035 - 1950 $\overset{o}{A}$

$\lambda_{air}(\overset{o}{A})$	$\nu_{vac.}(cm^{-1})$	Intensity [b]	v',v''	$\nu_{obs.} - \nu_{calc.}$
2034.85	49128	s	0,2	+1
2028.92	49272	w	1,3	+1
1998.50	50021	vs	0,1	+2
1993.66	50143	m	1,2	-1
1962.92	50928	vs	0,0	0
1958.70	51037	m	1,1	+3
1954.79	51140	w	2,2	-1
1950.83	51243	vw	3,3	-4

a: All bands are degraded to shorter wavelengths.

b: See footnote of Table II for abbreviations used.

TABLE XIII

Vibrational Scheme of the C → X System

v' \ v''	0		1		2		3	Mean $\Delta G'_{v+\frac{1}{2}}$
0	50928	907	50021	893	49128			
			1016		1015			1015.5
1			51037	894	50143	871	49272	
					997			997
2					51140			
3							51243	
Mean $\Delta G''_{v+\frac{1}{2}}$		907		893.5		871		

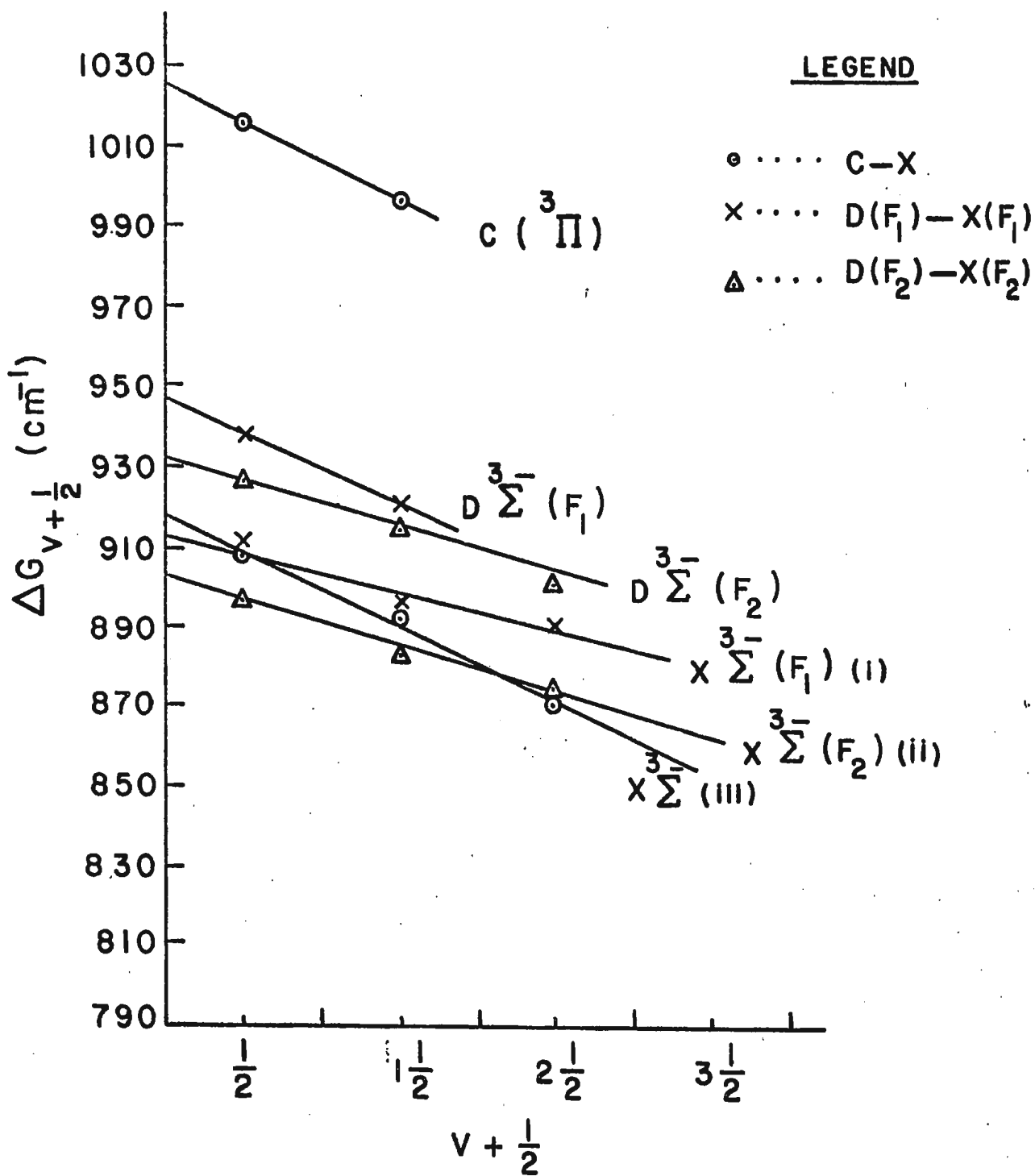Fig. 10. Plots of $\Delta G_{v+\frac{1}{2}}$ vs. $v+\frac{1}{2}$ For the C, D and X States of SeO . For the X State of the D - X System, Straight Lines (i) and (ii) Are Drawn From the $\Delta G_{v+\frac{1}{2}}$ Values Obtained From the Analyses of D $^3\Sigma^-(F_1)$- X $^3\Sigma^-(F_1)$ and D $^3\Sigma^-(F_2)$ - X $^3\Sigma^-(F_2)$ Sub-systems . The Straight Line (iii) Is Drawn From the X State of the C-X System .

The differences $\nu_{obs.} - \nu_{calc.}$ are also listed in the last column of Table XII. Our analysis of the C - X system is in general agreement with that of Haranath (1964). We tentatively assign the C - X system to the transition $^3\Pi_b - {}^3\Sigma^-$.

4.5 The D - X System:

The D - X System of SeO is shown in Plate VI. This system consists of two main groups of bands in the region 1980 - 1935 $\overset{o}{A}$ and its overall intensity is considerably weaker than that of the C - X system. Within each main group two sub-groups of bands are identified and the separations between the sub-bands with the same v',v" vary from 3.3 to 4.1 $\overset{o}{A}$. As stated earlier in Chapter 3, Barrow and Deutsch (1963) analyzed the rotational structure of the B $^3\Sigma^-$ - X $^3\Sigma^-$ system of SeO and found that the values of the spin splitting constant λ of the B and X states are 51 and 86.4 cm^{-1} respectively. When λ's are very large a given v',v" band in a $^3\Sigma^-$ - $^3\Sigma^-$ transition consists of two closely-lying sub-bands F_2-F_2 and F_3-F_3 and of a sub-band F_1-F_1 which is separated from the former by an amount $2(\lambda"-\lambda')$ approximately (for the bands of the B - X system these separations are approximately 75 cm^{-1}). In analogy with the B $^3\Sigma^-$ - X $^3\Sigma^-$ system of SeO, its D - X system is tentatively assigned to the transition $^3\Sigma^-$ - $^3\Sigma^-$. On this basis one expects two sub-systems for D - X:

(i) D $^3\Sigma^-(F_1)$ - X $^3\Sigma^-(F_1)$ and (ii) D $^3\Sigma^-(F_2,F_3)$ - X $^3\Sigma^-(F_2,F_3)$.

The wavelengths, wavenumbers, intensities and vibrational assignments of the two sub-systems of D - X are listed in Table XIV

TABLE XIV

Band Heads of the $D \rightarrow X$ System [a]

$\lambda_{air}(\overset{\circ}{A})$	$\nu_{vac.}(cm^{-1})$	Intensity [b]	v',v''	$\nu_{obs.} - \nu_{calc.}$ (cm^{-1})
		Sub-System $D\ ^3\Sigma^-(F_1) - X\ ^3\Sigma^-(F_1)$		
1974.23	50636	w	0,1	-2
1972.57	50679	vw	1,2	+2
1971.43	50708	vw	2,3	0
1939.37	51546	w	0,0	0
1938.34	51574	w	1,1	-2
1937.37	51600	w	2,2	+2

TABLE XIV (Continued)

Band Heads of the $D \to X$ System [a]

λ_{air}(Å)	$\nu_{vac.}$(cm^{-1})	Intensity [b]	v',v"	$\nu_{obs.} - \nu_{calc.}$ (cm^{-1})
		Sub-System $D\ ^3\Sigma^-(F_2,F_3) - X\ ^3\Sigma^-(F_2,F_3)$		
1978.39	50541	w	0,1	+4
1976.28	50584	w	1,2	+1
1974.72	50624	w	2,3	0
1973.60	50652	vw	3,4	-13
1943.42	51439	w	0,0	0
1942.33	51468	w	1,1	-1
1941.11	51500	w	2,2	+1
1940.16	51525	vw	3,3	-4

a: All bands are degraded to shorter wavelengths.

b: See footnote of Table II for abbreviations used.

and the vibrational scheme is shown in Table XV. The vibrational

constants ω_e, $\omega_e x_e$ and the system origin ν_e for each of the

sub-systems are determined in the manner described earlier for other

systems. The values of $\Delta G_{v+\frac{1}{2}}$ are plotted against the corresponding

$v+\frac{1}{2}$ values for the lower and upper states of each of the sub-

systems as shown in Fig. 10. The wavenumbers of the band heads of

the D - X system are represented by the following formulae:

For the sub-system $F_1 - F_1$:

$$(4-5) \quad \nu = 51528 + 955 (v' + \tfrac{1}{2}) - 8.5 (v' + \tfrac{1}{2})^2$$
$$- \{917 (v'' + \tfrac{1}{2}) - 4.5 (v'' + \tfrac{1}{2})^2\}.$$

For the sub-system $F_2, F_2 - F_3, F_3$:

$$(4-6) \quad \nu = 51424 + 938 (v' + \tfrac{1}{2}) - 5.5 (v' + \tfrac{1}{2})^2$$
$$- \{908 (v'' + \tfrac{1}{2}) - 5.5 (v'' + \tfrac{1}{2})^2\}.$$

The wavenumbers of the band heads are calculated by using the above

formulae and $\nu_{obs.} - \nu_{calc.}$ are listed in Table XIV. The

separations between the heads of the sub-bands for given v', v'' are

listed in Table XVI. The average value of these separations is 99 cm^{-1}

which is approximately equal to $2(\lambda'' - \lambda')$. Since $\lambda(=\lambda'') = 86.4$ cm^{-1}

for X $^3\Sigma^-$ (Barrow and Deutsch, 1963; also see Section 3.3 of this

thesis), $\lambda(=\lambda')$ for D $^3\Sigma^-$ is 37 cm^{-1} approximately.

TABLE XV

Vibrational Scheme of the D → X System

v'/v"	0		1		2		3		4	Mean ΔG'$_{v+\frac{1}{2}}$
0	51546(F₁)	910	50636(F₁)							
	107		95							
	51439(F₂)	898	50541(F₂)							
			938							938(F₁)
			927							927(F₂)
1			51574(F₁)	895	50679(F₁)					
			106		95					
			51468(F₂)	884	50584(F₂)					
					921					921(F₁)
					916					916(F₂)
2					51600(F₁)	892	50708(F₁)			
					100		84			
					51500(F₂)	876	50624(F₂)			
							901			901(F₂)
3							51525(F₂)	873	50652(F₂)	
Mean ΔG"$_{v+\frac{1}{2}}$		910(F₁)		895(F₁)		892(F₁)				
		898(F₂)		884(F₂)		876(F₂)		873(F₂)		

TABLE XVI

Separations Between the Heads of Sub-bands

of the $D \rightarrow X$ System

| v', v''	$\nu(F_1) - \nu(F_2, F_3)$ (cm^{-1})
0,1	95
1,2	95
2,3	84
3,4	--
0,0	107
1,1	106
2,2	100
3,3	--

4.6 Discussion:

(a) <u>Molecular Constants</u>:

A summary of the spectroscopic constants of all the known electronic states of SeO is presented in Table XVII. From this table it can be seen that the present study contributed greatly to the spectroscopic knowledge of the SeO molecule. The energy level diagram of SeO is presented in Fig. 11.

(b) <u>Electronic Configurations of SeO</u>:

The electron configuration of the atoms O, and Se are written as

$$O : K \ 2s^2 \ 2p^4$$
$$Se: KLM \ 4s^2 \ 4p^4 \ .$$
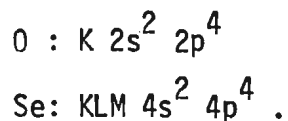
The electron configuration of the ground state of SeO is given by (Mulliken, 1932; Herzberg, 1950, Chapter VI)

(4-7) $KKLM \ (z\sigma)^2 \ (y\sigma)^2 \ (w\pi)^4 \ (x\sigma)^2 \ (v\pi)^2 \ ... \ ^3\Sigma^-, \ ^1\Delta, \ ^1\Sigma^+.$
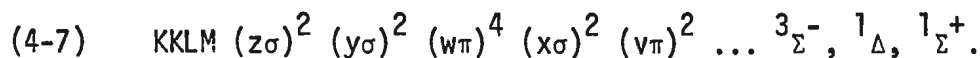
The expected low-lying upper electronic configurations are

(4-8) $KKLM \ (z\sigma)^2 \ (y\sigma)^2 \ (w\pi)^4 \ (x\sigma)^2 \ (v\pi) \ (w\sigma) \ ... \ ^1\Pi, \ ^3\Pi_r$

(4-9) $KKLM \ (z\sigma)^2 \ (y\sigma)^2 \ (w\pi)^4 \ (x\sigma) \ (v\pi)^2 \ (w\sigma) \ ... \ ^1\Sigma^+, \ ^1\Sigma^-, \ ^1\Delta, \ ^3\Sigma^+,$
$$^3\Sigma^-(2), \ ^3\Delta, \ ^5\Sigma^-$$
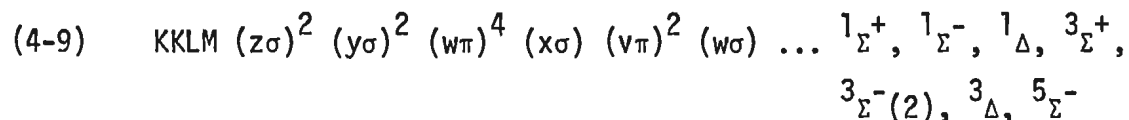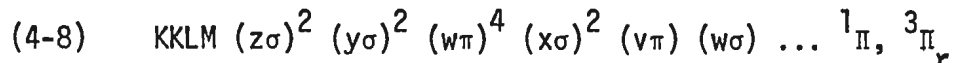
TABLE XVII

Molecular Constants of the SeO Molecule (cm^{-1})

State		T_e	ω_e	$\omega_e x_e$	B	α	$r(\overset{o}{A})$	λ	Observed Transition	Reference
y_2	y_1	+47830	974	6.0	-	-	-	-	$y_2 - y_1$	Present Work
y_1	y_1		906	21.0	-	-	-	-	-	"
x_2	x_1	+46009	993	2.0	-	-	-	-	$x_2 - x_1$	"
x_1	x_1		877	8.0	-	-	-	-	-	"
$D\ (^3\Sigma^-)$	F_2	51424	938	5.5	-	-	-	~37	D - X	"
	F_1	51356	955	8.5	-	-	-	"	D - X	"
$C\ (^3\pi)$		50874	1034	9.3	-	-	-	-	C - X	"
$c\ (^1\Sigma^+)$		43509	954	13.0	-	-	-	-	c - b	"
$B\ ^3\Sigma^-$	F_2	34012.2*	$\Delta G_{\frac{1}{2}}=517.7$	-	$B_0=0.3391$	-	$r_0=1.931$	-	B - X	Barrow & Deutsch (1963)
	F_1	33910	522.3	3.9	$B_0=0.3332$	-	-	$\lambda_0=51$	"	"
$b\ (^1\Sigma^+)$		9570.7	834.9	5.5	-	-	-	-	b - X	Present Work
$a\ (^1\Delta)$		9518.4*	-	-	-	-	-	-	a - X	"
$X\ ^3\Sigma^-$	F_2	0.0	915.43	4.52	$B_e=0.4705$	0.0033	$r_e=1.640$	-	-	Barrow & Deutsch (1963)
	F_1	-172	914.69	4.52	$B_e=0.4655$	0.0032		$\lambda_0=86.4$	-	"

* T_{00} Values.

In addition to the systems shown here, two brief systems x_2-x_1 and y_2-y_1 occur in the region 44360-48100 cm^{-1}. The constants of these systems are given in Table XVII.
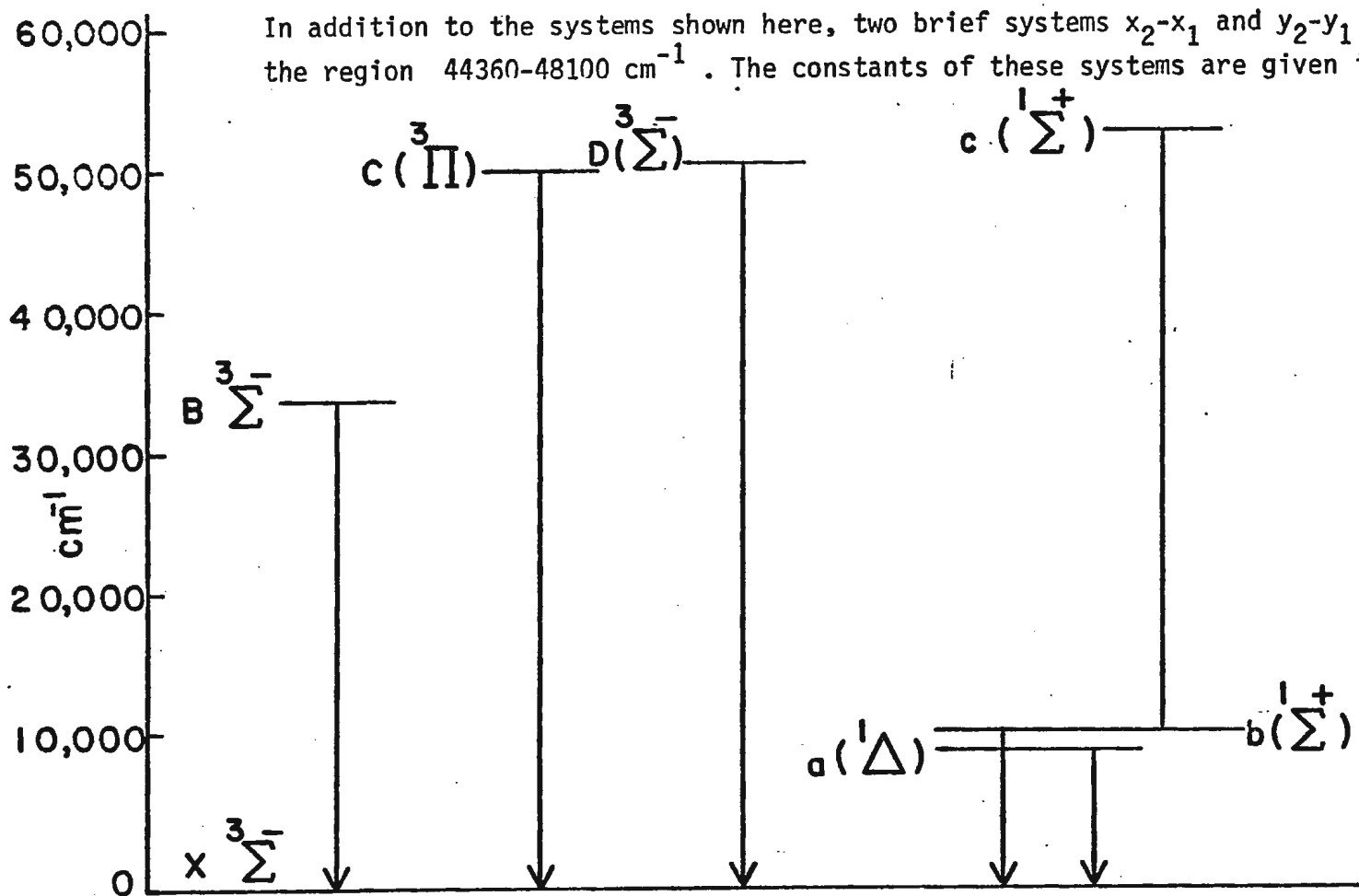
Fig. 11. Energy Level Diagram of SeO.

(4-10)   KKLM $(z\sigma)^2$ $(y\sigma)^2$ $(w\pi)^4$ $(x\sigma)$ $(v\pi)^3$ ... $^1\Pi,$ $^3\Pi_i$.

Further higher electron configurations involve excitation from the $(w\pi)^4$ orbital and require somewhat more energy than the configurations given above. The three states resulting from the ground electronic configuration $\sigma^2\pi^2$ are attributed to $X\ ^3\Sigma^-$, a $^1\Delta$, and b $^1\Sigma^+$ states (see Chapter 3). States $c(^1\Sigma^+)$, B $(^3\Sigma^-)$ and D $(^3\Sigma^-)$ probably belong to the configuration (4-9) and state C $(^3\Pi)$ belongs to configuration (4-8) or (4-10). States x_1, x_2, y_1 and y_2 may also belong to the configurations (4-8) to (4-10).

ACKNOWLEDGMENTS

The author is deeply indebted to his supervisor, Dr. S.P. Reddy, for his help, encouragement and guidance.

Special thanks is due to Dr. S. W. Breckon for his interest in this research.

The author is grateful to Dr. N. Rich for helpful discussions. He is also thankful to Mr. R. D. G. Prasad for his help in the preparation of plates and figures. Mr. R. Alexander, Mr. R. Tucker and Mr. D. Seymour deserve special thanks for their skilful photography, draftsmanship and glassblowing, respectively. The assistance from the technical personnel of the Physics Department is highly appreciated.

The author is highly grateful to his wife, Marcella, for her patience and for typing the thesis and doing some calculations.

REFERENCES

ALI, M. K. 1969. M.Sc. Thesis, Memorial University of Newfoundland.

AMANO, T., HIROTA, E., and MORINO, V. 1967. J. Phys. Chem. Japan,
        22, 399.

ASUNDI, R. K., JAN-KHAN, M., and SAMUEL, R. 1936. Proc. Roy. Soc. A,
        157, 28.

BABCOCK, H. D., and HERZBERG, L. 1948. Astrophys. J., 108, 167.

BARROW, R. F., and DEUTSCH, E. W. 1963. Proc. Phys. Soc. 82, 548.

CARRINGTON, A., LEVY, D. H., and MILLER, T. A. 1966. Proc. Roy.
        Soc. (London), Ser. A, 293, 108.

CARRINGTON,A., CURRIE,G.N., LEVY, D.H., and MILLER, T.A. 1969.
        Molec. Phys. V 17 , NO 5, 535 .

CHOONG, S.-P. 1938. Ann. Phys., Paris, 10, 173.

COLLIN, R. 1968. Can. J. Phys. 46, 1539.

COLLIN, R. 1969. Can. J. Phys. 47, 979.

DOUGLAS, A. E. and JONES, W. E. 1966. Can. J. Phys. 44, 2251.

EDLEN, B. 1953. J. Opt. Soc. Amer. 43, 339.

FINDLAY, F. D. 1970. Can. J. Phys. 48, 2107.

HARANATH, P. B. V. 1964. J. Mol. Spectros. 13, 168.

HARANATH, P. B. V. 1965. Indian. J. Pure and Applied Phy. Vol. 3, 75.

HERZBERG, G. 1950. Spectra of Diatomic Molecules, 2nd ed.
        (D. Van Nostrand, Princeton, New Jersey).

HERZBERG, G. 1968. Mem. Soc. Roy. Sci. Liege Collect. 16, 121.

HERZBERG, G. and HUGO, J. T. 1955. Can. J. Phys. 33, 757.

HERZBERG, L. and HERZBERG, G. 1947. Astrophys. J. 105, 353.

HYNES, D. L. 1968. B.Sc. Honours Dissertation, Memorial University
     of Newfoundland.

ROSEN, B. 1970. International Tables of Selected Constants:
     Spectroscopic Data Relative to Diatomic Molecules
     (Pergamon Press, New York).

SCHLAPP, R. 1932. Phys. Rev. 39, 806.

TOWNES, C. H. and SCHAWLOW, A. L. 1955. Microwave Spectroscopy
     (New York: McGraw-Hill).

WOOD, R. W. 1952. Physical Optics, 3rd ed. (The Macmillan Company,
     New York).

GENERAL REFERENCES

ALBERTI, F., ASHBY, R. A. and DOUGLAS, A. E. 1968. Can. J. Phys.
46, 337.

GATTERER, A. and JUNKES, J. 1956. Arc Spectrum of Iron, 2nd. ed.
(Specola Vaticana, Citta del Vaticano).

HARRISON, G. R. 1939. M. I. T. Wavelength Tables. (John Wiley
and Sons, New York).

HARRISON, G. R., LORD, R. C. and LOOFBOUROW, J. R. 1948. Practical
Spectroscopy (Prentice-Hall, New York).

HERZBERG, G. 1950. Spectra of Diatomic Molecules, 2nd. ed.
(D. Van Nostrand, Princeton, New Jersey).

JONES, W. E. 1967. Can. J. Phys. 45, 21.

MULLIKEN, R. S. 1928. "The Assignment of Quantum Numbers for Electrons
in Molecules. II. Correlation of Molecular and Atomic
Electron States", Phys. Rev. 32, 761.

MULLIKEN, R. S. "Interpretation of Band Spectra",
Parts I, II(a) and II(b), Rev. Mod. Phys. Vol. 2 (1930)
Part II(c),   "   "   "   Vol. 3 (1931)
Part III,   "   "   "   Vol. 4 (1932)

SAWYER, R. A. 1951. Experimal Spectroscopy, 2nd. ed. (Chapman and Hall,
London).

SHENSTONE, A.G. 1955. J. Opt. Soc. Am. 45, 868 .